# Linear-Cross and Linear-Circular Polarization Converter in the THz Regime

**PROJECT REPORT**

*Submitted in partial fulfillment of the requirements for the award of the Degree of Master of Technology in Electronics and Communication Engineering with specilisation in Communication Systems by the A P J Abdul Kalam Technological University*

*by*

**TEJAS S**

**TKM20ECCS14**


**DEPARTMENT OF ELECTRONICS AND COMMUNICATION ENGINEERING**

**TKM COLLEGE OF ENGINEERING**

**KOLLAM 691 005**

**2022**

**DEPARTMENT OF ELECTRONICS AND COMMUNICATION ENGINEERING**

**TKM COLLEGE OF ENGINEERING**

**KOLLAM 691 005**

## CERTIFICATE

Certified that this thesis titled **"Linear-Cross and Linear-Circular Polarization Converter in the THz Regime"** is a bonafide record of the work done by **TEJAS S** (Reg. No. TKM20ECCS14) under my supervision, in partial fulfillment of the requirements for the award of the Degree of Master of Technology in Electronics and Communication Engineering with specialization in Communication Systems by the A P J Abdul Kalam Technological University.

**Guide**
**Dr.NISSAN KUNJU**
Assistant Professor
Dept. of ECE, TKMCE

**Coordinator**
**Dr.NISHANTH.N**
Associate Professor
Dept. of ECE, TKMCE

**HoD**
**Prof.ABID HUSSAIN**
Dept. of ECE
TKMCE

# Acknowledgement

On the very outset of this report, I would like to extend my sincere and heartfelt obligation towards all the personages who have helped me in this endeavor. Without their active guidance, help, cooperation and encouragement, I would not have made headway in this project.

I am ineffably indebted to my guide Dr.Nissan Kunju,Assistant Professor in Electronics and Communication Engineering who stood with me giving valuable suggestion, new ideas and also guidance in preparing this project. I thank my coordinator,Dr.Nishanth N, Associate Professor in Electronics and Communication Engineering Department for giving constructive criticism, encouragement and expert supervision in all spheres of the work.

I gratefully acknowledge the contribution and guidance from Dr. Sukomal Dey, Assistant Professor, Dept. of EEE, IIT, Palakkad, and Mr. Mohammed Abdul Shukoor, Research Scholar, Dept. of EEE, IIT, Palakkad for guiding me and for giving valuable contribution.

I sincerely thank Prof. Abid Hussain M, Head of the Department for providing necessary information regarding the project and also his support.I must express my gratitude to all the staff members of Electronics and Communication Engineering Department.

I also acknowledge with a deep sense of reverance , my gratitude towards my parents, who stood with me during my ups and downs.

Last but not least gratitude goes to all my friends who directly or indirectly helped me to do this work.

TEJAS S

# ABSTRACT

The design of novel reflective type multiband dual polarizers is proposed in this dissertation. The proposed structures can perform linear to cross as well as linear to circular conversion in the THz regime. The designed structures consist of a thin gold coated Frequency Selective Surface (FSS) printed on top of a polyamide substrate, with a thin gold film as the ground plane.

The square loop FSS exhibits Linear-Circular conversion with an Axial Ratio ($\leq$ 3dB) from 0.49-0.50 THz, 0.60-0.83 THz, 1.16-1.62 THz and 1.81-1.85 THz. In addition, it also performs the Linear-Cross conversion with a minimum 90% Polarization Conversion Ratio (PCR) from 0.53-0.56 THz, 0.92-1.07 THz and 1.69-1.75THz. The polarizer unitcell architecture is compact with structural dimensions of $0.121\times0.121\times0.041$ $\lambda_L^3$, where $\lambda_L$ is the lowest operating frequency's free-space wavelength.

The circular loop FSS shows Linear-Cross conversion with a minimum 90% Polarization Conversion Ratio (PCR) from 0.62- 0.65THz, 0.98-1.10THz and 1.74-1.80THz. Furthermore it perform Linear-Circular conversion with Axial Ratio ($\leq$ 3dB) from 0.58-0.59THz, 0.69-0.90THz, 1.18-1.67THz and 1.87- 1.90THz. This unitcell has a structural dimensions of $0.153\times0.153\times0.039$ $\lambda_L^3$, where $\lambda_L$ is the lowest operating frequency's free-space wavelength.

Multiple surface plasmonic resonance is the phenomenon behind the conversion at different frequency bands. The metasurface's performance is stable up to $45^0$ for both Transverse Electric (TE) and Transverse Magnetic (TM) oblique incidences. Making this design compact, with angular stable multi-band multi conversion ability that will significantly impact the THz applications in real-time.

# Contents

# List of Figures

# List of Tables

# Abbreviations

| | |
|---|---|
| AR | Axial Ratio |
| ECR | Energy Conversion Ratio |
| EM | Electromagnetic radiation |
| EF | Electric Field |
| FSS | Frequency Selective Surface |
| LC | Linear to circular |
| LX | Linear to cross |
| MF | Magnetic Field |
| PC | Polarization Converter |
| PCR | Polarization Conversion Ratio |
| TE | Transverse Electric |
| THz | TeraHertz |
| TM | Transverse Magnetic |

# Chapter 1

# Introduction

The electric field and magnetic field interplay each other to create the electromagnetic waves [1]. Polarization is one of the paramount factors of EM waves, it has been widely used in electromagnetic communication, imaging [2], detection, spectroscopy and biosensing. The THz regime having a large potential still remains unexplored. Neoteric developments in the THz realm led to buildout in fields like imaging, short range communication systems and defense applications. Devices such as lenses, absorbers and sensors working in THz regime are yet to be discovered [3]–[6], owing to limited sources and detectors at these frequencies.

Manipulation of EM waves is an inescapable link in different fields like satellite communication, mobile communication and so on. The manipulation of these EM waves can be attained using the Polarization convertors. Polarization conversion can be realized using birefringence effect, dichronic crystals and optical gratings. They suffer from limitations such as narrow bandwidth, bulkier volume [7]–[9] and cannot be used for long distance transmission. These hindrances lead to evolution of metamaterial-based polarization convertors which can even work in the negative refractive index. The shape,geometry,size and orientation metameterials plays a significant role to manage the flow of electromagnetic waves.These materials are arranged in repeating or in periodic patterns, at levels that are lower than the wavelength they intract with.

Metasurface based polarization control devices, owing to small size, high efficiency and easy integration, are widely used polarization conversion, optical rotators and asymmetric transmission.

Metasurface based polarization converters are made of either chiral or anisotropic geometry [10,11]. The main drawback related to these geometry is the limited bandwidth. The most common methods to enhance the bandwidth of metasurface-based devices is the use of stacked layers,multiresonance and fractal geometry in the design [12–16]. In a multi-resonance method structure, multiple unit cells are arranged within a single cell to create super cells, while in layeres structures, layers are stacked, one on top of the other, to create a device. Despite their complexities and high costs, these techniques are not practical for practical applications. As such, a strong need remains to develop metasurface-based wideband polarizers that are compact, miniaturized, simple and cost-effective. Key findings of this work includes linear-cross and linear-circular polarization converters which is angular stable, capable of worksing in the THz regime.

## Objectives

- Design metamaterial based linear-cross and linear-circular polarization converters.
- Evaluate performance of the designed polarization converters in the THz regime.

## Organization of the thesis

The first chapter of the thesis introduces the concept of metamaterials and the drawbacks of conventional polarization converters. The second chapter includes a comprehensive review of the literature covering the broad area of polarization converters. The third chapter focuses on the evolution of unit cell design based on the drawbacks of the designed structures. The fourth chapter details the results and discusses the interpretations and findings. The last chapter deals with the conclusion followed by references and appendix.

# Chapter 2

# Literature Review

Thanh Nghi et al.[17] discuss a cross polarization converter is numerically designed.The designed structure is a reflective type fig(2.1). A split ring metal pattern is used as patch. The dielectric medium is $VO_2$. This polarization converter convert linearly polarized waves in the range 2.98THz-4.16THz to circular polarized waves. One of the limitation with this structure is $VO_2$ is sensitive to temperature as a result the frequency of operation can change.

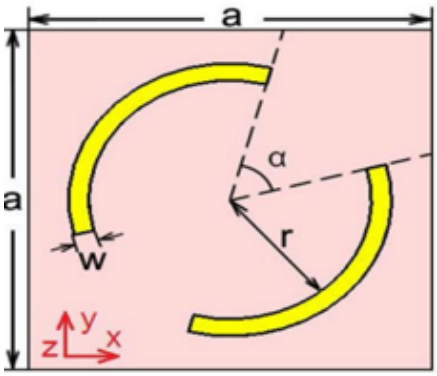


Figure 2.1: Split ring circular polarization converter

Linear-to-circular reflective type Polarization Converter Utilizing Double-arc-based structure fig(2.2) was mentioned in literature by Jing Zhao,Yannan Jiang[18]. It converts the incoming linear polarized wave is given a phase shift of $90^0$. The polarization conversion efficency is low for this design. FR-4 is used as substrate which act as a lossy material as the frequency of operation increases. It works in the frequency range 0.59THz-1.30THz.

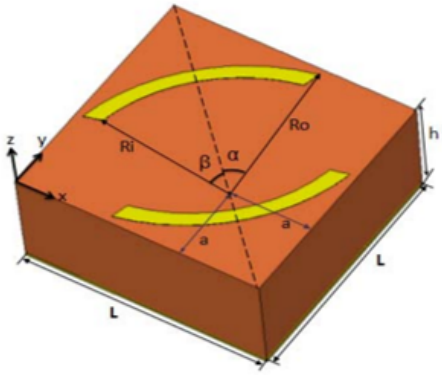


Figure 2.2: Split ring circular polarization converter

A L shaped metasurface based polarization converter is designed by Feng luo et al.[19]. This structure can convert the linear polarized wave to cross polarized waves. A split square ring act as patch and bandwidth very low. It can convert multiple frequencies. An asymmetric dual band linear to circular polarization converter is designed in Xiangjun et al.[20]. The structure follows a chiral geometry ie; mirror image and original image are different. Due to this chiral geometry the bandwidth is very narrow. Dielectric material used is FR-4 which is a lossy material.

A. K. Baghel et al.[21] mentioned about a structure that has the ability to convert the linear polarization into cross polarized waves. The substrate used to make the structure is RT Roger. The cost of RT Roger is more compared to other dielectric materials.The designed structure can only convert a single frequency ie; 8.8GHz. There are already many other polarization converters that work in the GHz regime.

Bao-qin Lin et al.[22] raises an eight shaped linear to circular polarization converter. Polarization conversion takes place between 6.78GHz-23.70GHz. Due to the structural complexity it is difficult to fabricate.

A broadband polarization converter for terahertz waves is proposed by Pan Wu et al.[23]. Linear polarized wave is converted to circular polarized. Polarization takes place at $\pm n\frac{\pi}{2}$ multiples. The split ring shaped patch is shown in fig(2.3)

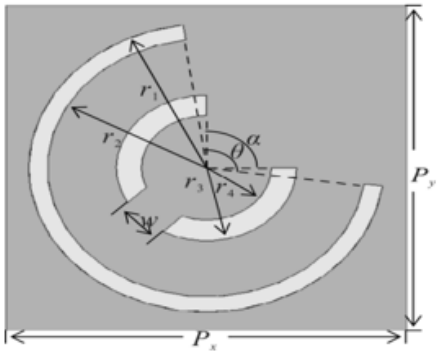


Figure 2.3: Broadband circular polarization converter

Manipulation of polarization is essential for radar communication and other applications. EIT is a coherent optical non linearity that gives a narrow spectrum as output. Zhu L et al.[24] intoduces a dielectric material used to make patch over the substrate is having different shapes. Due to variation in shapes the polarization conversion efficiency is low. The losses produced by dielectric material is larger compared to meta surface based polarization converters.

Graphene is one of the easily available isotrope of carbon which is used to make the patch.Shakib Quader et al.[25] proposes a three layered reflective type polarization converter. The frequency of operation can be altered by changing the applied voltage to the graphene structure. The main drawback is fabrication is difficult.

A Broad band polarization converting meta surface for C and X band application is proposed by Babar,Jingdong[26]. The linear polarized waves is transformed into circular polarized wave. The square patch is made on top of the substrate RT Roger. This converter can convert the frequencies coming in the range 5.9GHz–10GHz to circular polarized wave, when we use chiral or anisotropic structure the bandwidth will be limited. The square resonator produce harmful electromagnetic interference.

Muhammad Abdul Shukoor, Sukomel Dey[27] mooted a Wideband Dual-Cut Circular Ring based Linear Cross and Linear-Circular Polarizing Reflector is designed. This polarization converter is capable of converting linear polarized wave to linear and linear to circular in multiple frequency bands. The frequency selective surface is printed on top of FR-4 substrate which may become lossy at high frequency. The ground plane and patch is made of copper which will act as a resistive material as the frequency increases. The designed structure is shown in fig(2.4).

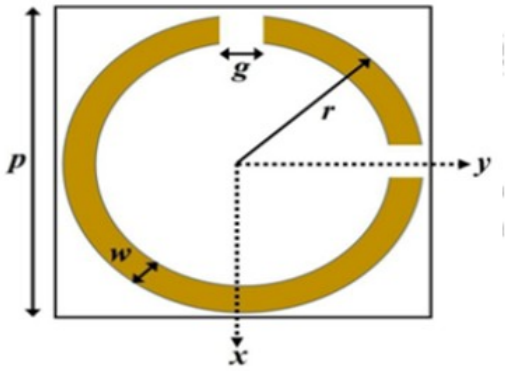


Figure 2.4: split Ring linear to circular polarization converter

R.M.H. Bilala et al.[28] discusses about a polarization converter working in the THz regime that can convert linear polarised wave to cross as well as linear polarized wave to circular. Works in the frequency range 1Thz-4THz. A fractal H shaped structure is the patch. Due to the fractal shape the bandwidth will be high. It is a three layered structure in which $SiO_2$ is the dielectric material. The patch and ground is made of gold, it act as a reflective type polarization converter. One of the limitation with this structure is that when linear polarized wave is converted to circular there will be noise present in the output. The designed structure is shown in fig(2.5)

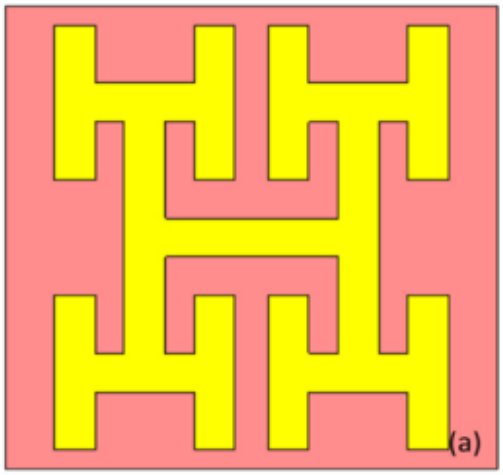


Figure 2.5: Fractal H shaped polarization converter

M. Ismail Khan et al.[29] mentions about anisotropic metasurfaces used to make the polarization convertor. Anistropic materials have special properties ie, the polarization can be controlled by electric field or magnetic field. A double headed arrow design and split ring resonator is used to increase the bandwidth. The substrate used is FR-4 and metallic part is made of copper. FR-4 which will become lossy as the frequency increases. First a unit cell with a square patch that works at 7.5GHz is designed. But this structure does not have any polarization conversion ability. The design is modified so that it becomes an asymmetric structure. Polarization conversion can be achieved only by an asymmetric structure.

Here poly tetra fluoroethylene is used to make the dielectric material. Thanh Nghi et al.[30] designed a structure that can convert linear polarized waves to cross polarized waves ie; at $\pm n\pi$ multiples. The patch and ground is made of gold. The patch consist of two disks and a double-headed axe structure. But the polarization conversion ratio associated with this structure is very low. The proposed structure is shown in fig(2.6).

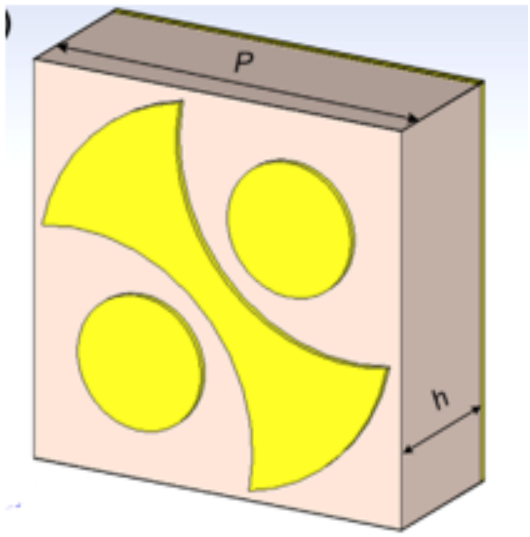


Figure 2.6: Double headed axe polarization converter

Xu et al.[31]. proposed a split ring-based polarizer that converts the linearly polarized wave to its orthogonal while reflection with a minimum 80% Polarization Conversion Ratio (PCR)from 0.49 to 1.88 THz (1.39 THz bandwidth). An ultrathin bi-layered metasurface is proposed to achieve wideband linear-circular polarization conversion

in X and Ku-band applications [32]. An ultrawideband highly efficient linear-circular polarizer is proposed with a relative bandwidth of 80% using a double split square resonator [33]. The polarization converter's performance tunability is achieved with graphene at THz frequencies [34]. By electrically regulating the Fermi energy of the graphene sheets, the proposed device may dynamically transition its capabilities between linear-to-linear, linear-to-circular, and linear-to-elliptical polarization conversion in broadband without reoptimizing and refabricating the structures [35]. With the use of a biassing device, they could result in bulky setups and considerable loss. Furthermore, Mahdi et al. proposed an ultra-wideband reflection-mode linear-circular polarization converter for application in the terahertz realm [36]. A dual-slotted circular ring compact multi-band linear-circular and linear-cross THz polarizer is proposed by [37]. Nonetheless, this design is not ideal for low profiles because of the multi-layer construction. linear-circular polarization converters working in the terahertz zone, which have wide band features, high efficiency, and low profile, have been underutilized, as previously indicated.

# Chapter 3

# Design and Simulation

The polarization of an electromagnetic wave describes the amplitude and direction of the wave's electric field. Electromagnetic waves, such as visible light and microwaves,have orthogonal electric and magnetic fields that run in opposite directions from the wave's propagation path. Polarization conversion is achieved by controlling and manipulating the states of electromagnetic (EM) waves polarization. In the polarized wave the direction and magnitude of vibrating electric field are related.

The performance of this proposed structures in the THz range is investigated using the commercial software Ansys HFSS with a frequency domain solver. A single unit is irradiated by a plane THz wave propagating along the z-axis, with electric feld parallel to the x-axis and magnetic feld parallel to the y-axis. Periodic boundaries are applied in the x and y directions and an open boundary condition is used in the z direction.The opposite faces of the region was made perfect electric conductor and perfect magnetic conductor so that the EF and MF interact with each other. Flouqet port was used to analyse the structure. Flouqet port is assigned because this unitcell is going to be part of a array of unitcells. This flouqet port will help to analyse how the unit cell will behave when they are cascaded together.

When a y polarized wave is incident on the metasurface, the cross-polarized wave is defined by $r_{xy} = |E_{xr}|/|E_{yi}|$ and the co-polarized wave by $r_{yy} = |E_{yr}|/|E_{yi}|$.Here $|E_x|$ and $|E_y|$ are the magnitudes of electric fields in x and y direction. The incident and reflected components are denoted by i and r. For any linear to cross polarization converter, its ability is defined by the Polarization Conversion Ratio (PCR) [38] given

as,

$$PCR = \frac{|r_{xy}|^2}{|r_{xy}|^2 + |r_{yy}^2|} \tag{3.1}$$

PCR should be above 90% for the frequencies at which linear to cross polarization conversion takes place.

The circular polarization efficiency of the polarization converter can be determined using the axial ratio(AR)[39]. The AR should be less than 3dB.Calculated as,

$$R = \frac{r_{xy}}{r_{yy}} \tag{3.2}$$

The incoming waves may not always be normal to the metasurface, as the surface impedance variation is not same. Hence the variation of PCR and AR should be stable for different incidence angles.

## 3.1 Square ring edge square PC

A $SiO_2$ based reflective type polarization converter is designed. The designed structure has the ability to convert linear-cross and linear-circular polarization. The designed unit cell is shown in fig(3.1). The periodicity of unit cell P=60$\mu m$,w =4$\mu m$, h =10$\mu m$ and S =10$\mu m$. The bottom gold plate and top FSS has a dimension $t = 0.2\mu m$.

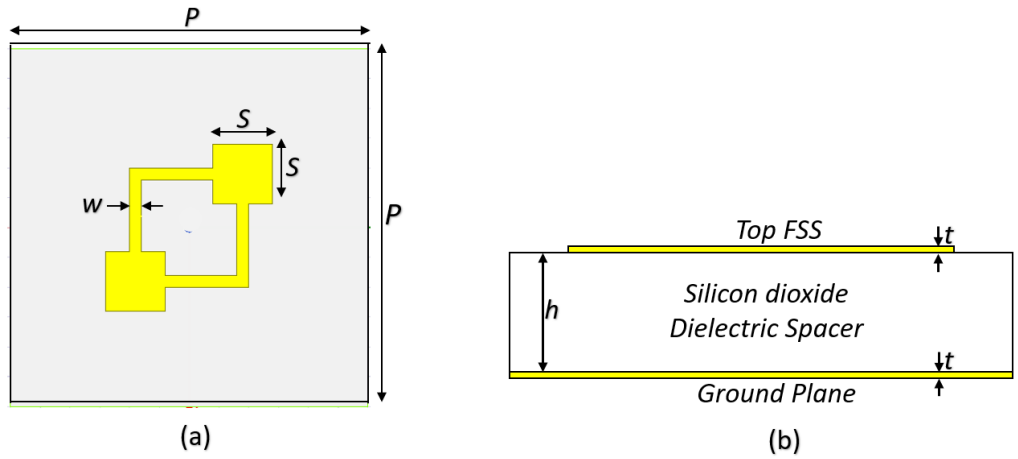


Figure 3.1: (a) Top and (b) side view of the square ring edge square polarizer.

## Performance analysis

The simulated reflectance and PCR graph is shown in fig(3.2a) and fig(3.2b) it's clear that the PCR is below 90% so this structure cannot achieve linear to cross conversion.

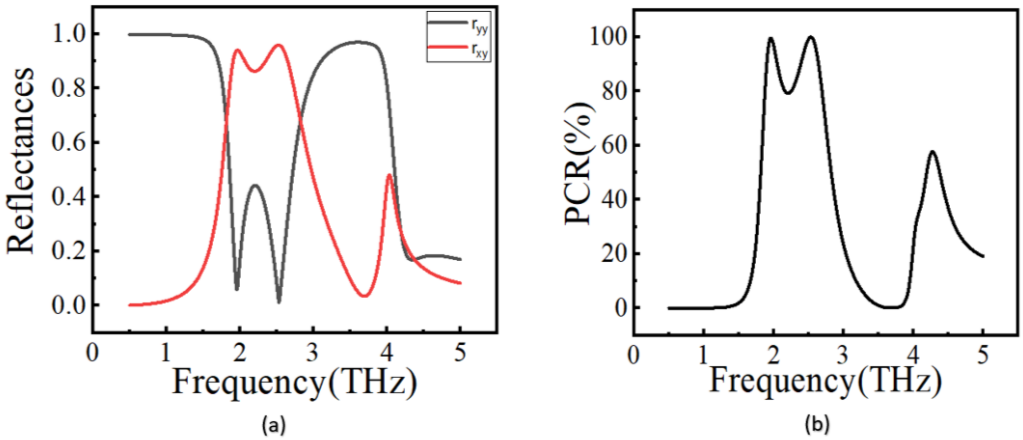


Figure 3.2: Simulated reflectances (a) magnitudes and (b)PCR

## 3.2 Split ring PC

The proposed design is a reflective polarization convertor. Schematic of the unit cell of the proposed polarization convertor is shown in Fig(3.3). This convertor is capable of both linear-cross and linear to circular polarization conversion simultaneously in multiple frequency bands at terahertz frequency range. Here $SiO_2$ is used as the substrate. The ground and top FSS are made of gold with a thickness, t =0.2$\mu m$. The finalized dimensions of the unitcell are P = 60m,w =3m and h =10m, as shown in fig(3.3)

## Performance analysis

From the reflectance characteristics, fig(3.4a) it can be seen that linear-cross and linear-circular polarisation conversion is achieved in multiple frequency bands. The PCR was above 90% during linear-cross polarization conversion as in fig(3.4b). Axial Ratio for linear-circular polarization was also below 3dB mark, fig(3.4c). The incident

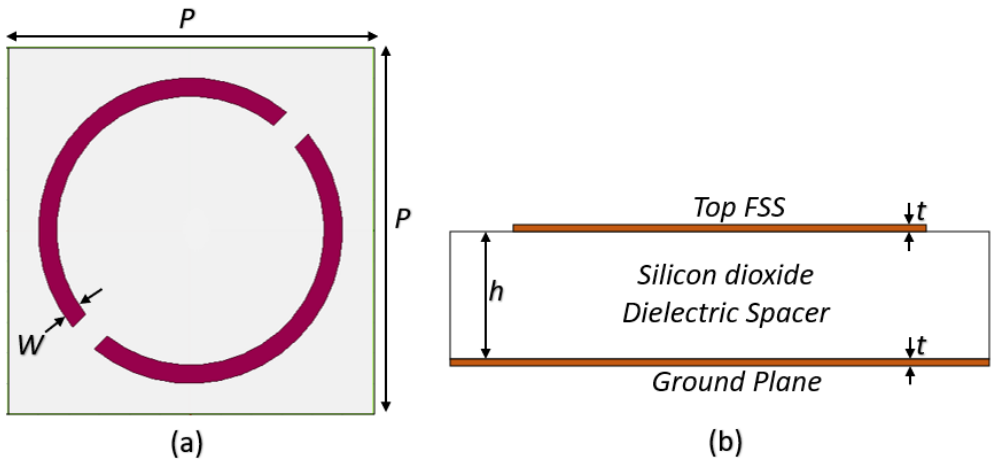


Figure 3.3: (a) Top and (b) side view of the split ring polarizer.

wave can strike the unit cell at different incidence angles, the designed structure should be angular stable. The PCR was stable upto incidence angle $45^0$,fig(3.5a). However the axial ratio was not stable,fig(3.5b). Hence this structure cannot be used for practical applications.

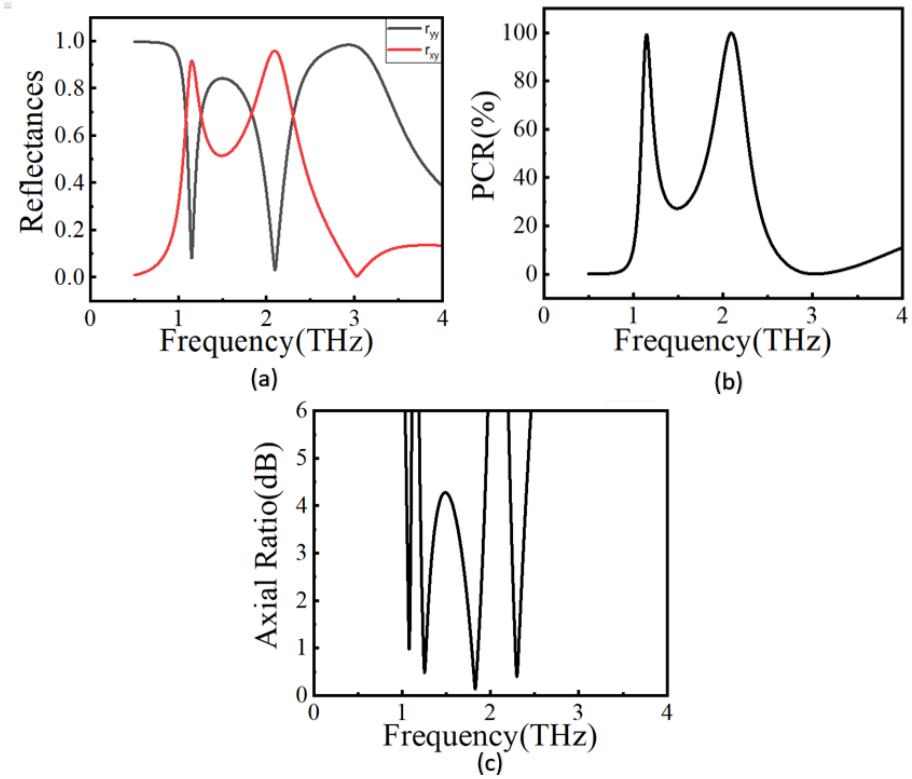


Figure 3.4: Simulated reflectances (a) magnitudes,(b)PCR and (c)AR.

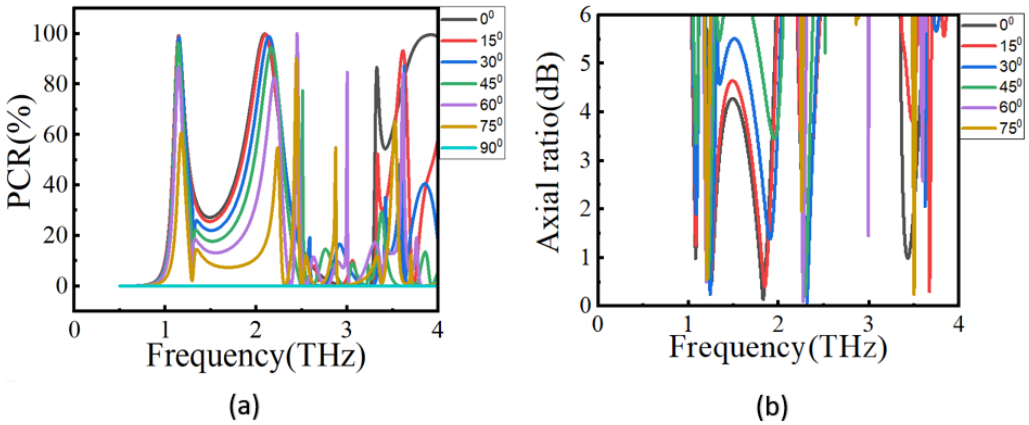


Figure 3.5: Simulated (a)PCR and (b)AR(dB) for different angles.

## 3.3 Double split ring PC

A dual split ring structure is designed with gold as ground and top FSS with a thickness t =0.2$\mu m$. The dielectric material is $SiO_2$, having a height h =10$\mu m$. Schematic of the designed structure is shown in fig(3.6). Here P=60$\mu m$ and w =2$\mu m$.

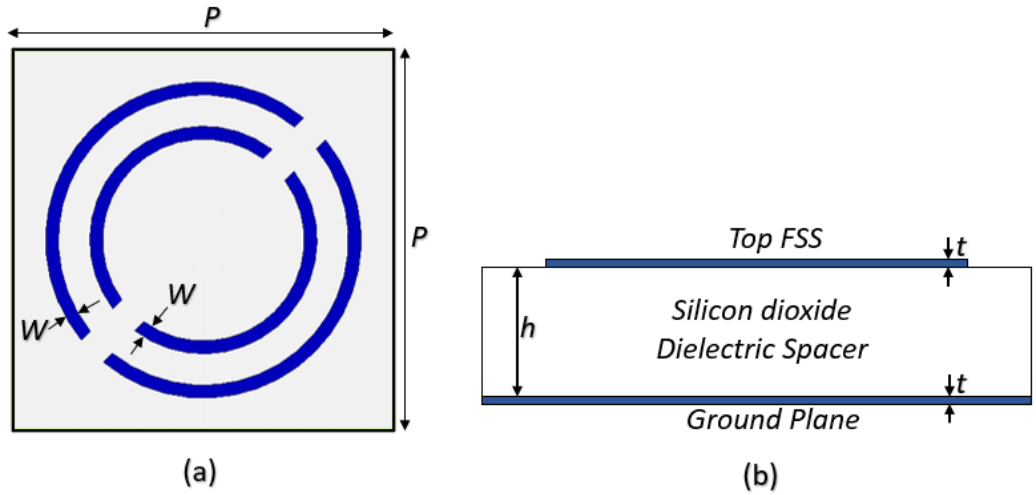


Figure 3.6: (a) Top and (b) side view of the double split ring polarizer.

## Performance analysis

The simulated reflectance and PCR graph is depicted in given in fig(3.7). Linear to cross conversion cannot be achieved by the given structure as the PCR is below 90% for the frequencies.

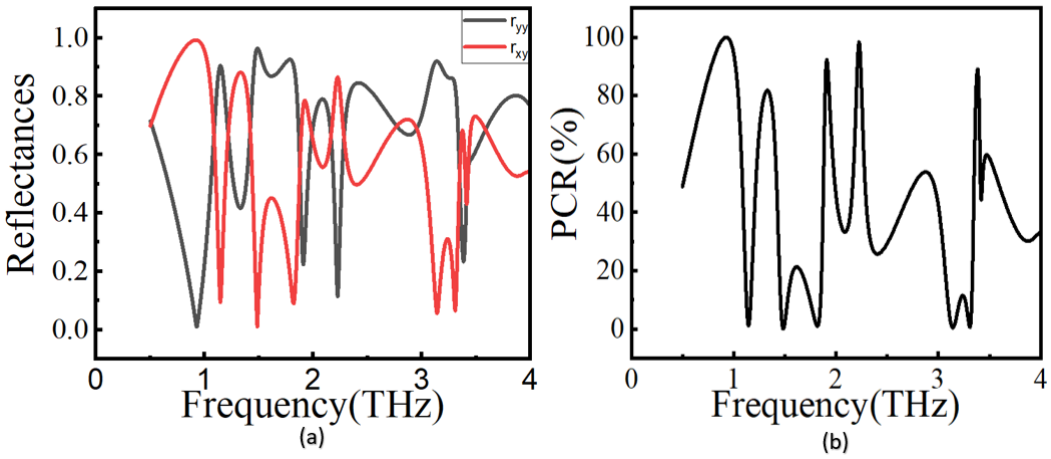


Figure 3.7: Simulated reflectances (a) magnitudes and (b)PCR.

## 3.4 Double quarter ring PC

A reflective type polarization converter working in the THz regime is designed, shown in fig(3.8). The top FSS and ground plane is made of gold with a thickness, t =0.2$\mu m$. The structure poses multiband linear-circular and linear-cross conversion abilities. The $SiO_2$ substrate has a height,h = 10$\mu m$ also P =10$\mu m$ and w =2$\mu m$.

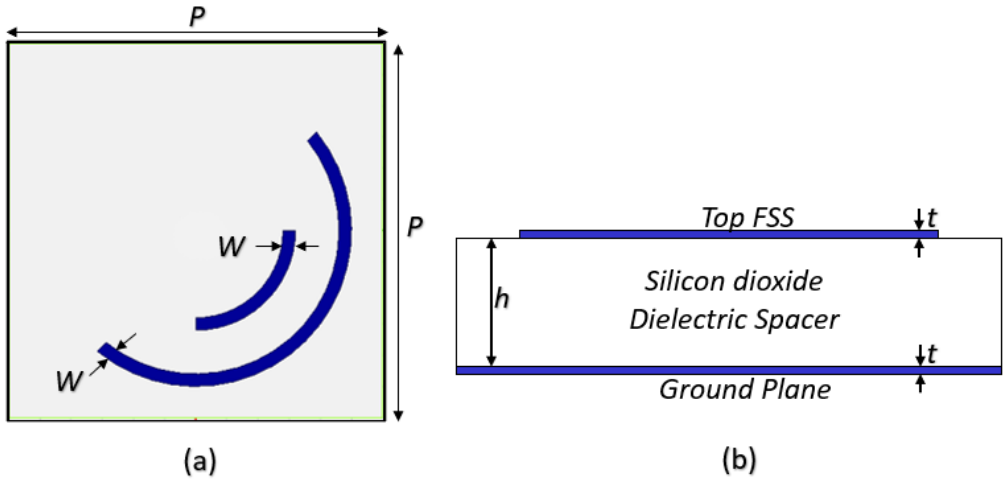


Figure 3.8: (a) Top and (b) side view of the double quarter ring Polarizer.

## Performance analysis

Polarization conversion is attained in the THZ regime. The relectances graph is depicted in fig(3.9a). The PCR was above 90% for linear-cross polarization, fig(3.9b).

AR for linear-circular polarization is also below 3dB,fig(3.9c). The main constrain of this design is that the bandwidth in which conversion occurs is very small.

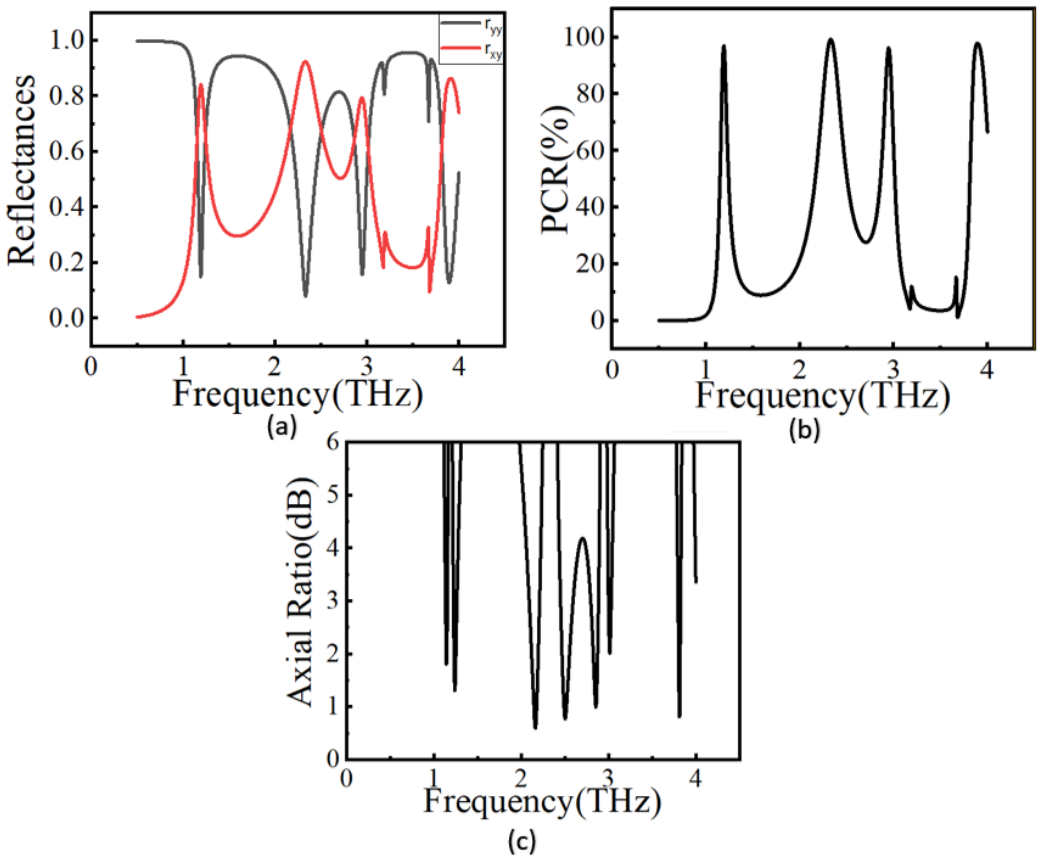


Figure 3.9: Simulated reflectances (a) magnitudes (b)PCR and (c)AR.

## 3.5 Three square loop PC

The top FSS is printed on the top of the commercially available silicon dioxide ($SiO_2$) substrate, having a thickness, h =10$\mu m$. The substrate is terminated with the ground on the other side. An 0.2$\mu m$ thin gold film is used as the metallic layer for the top FSS and the ground. The periodicity of the unitcell P =60$\mu m$, w =4$\mu m$ and Y =20$\mu m$. The proposed structure is shown in fig(3.10)

## Performance analysis

The designed structure can perform linear-cross and linear-circular polarization conversions in the THz regime. The reflectances magnitude graph is given in fig(3.11a).

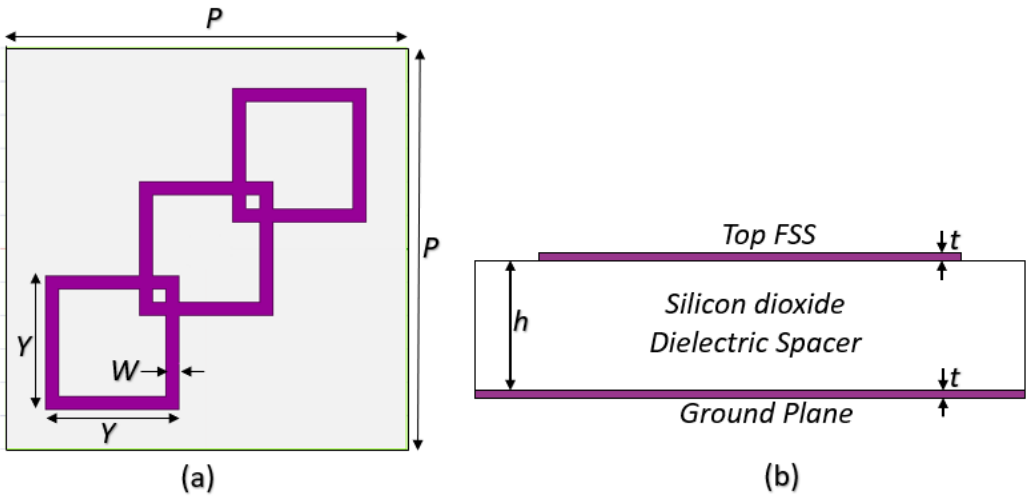


Figure 3.10: (a) Top and (b) side view of the three square loop polarizer.

The performance of linear-circular conversion efficiency is calculated from the axial ratio which should be less than 3dB line,fig(3.11c). The PCR was also above 90% for the frequencies in which linear-cross polarization takes place, fig(3.11b). Neverthless the structure was not angular stable, from fig(3.12a) the PCR was not angular stable making it unsuitable for practical applications.

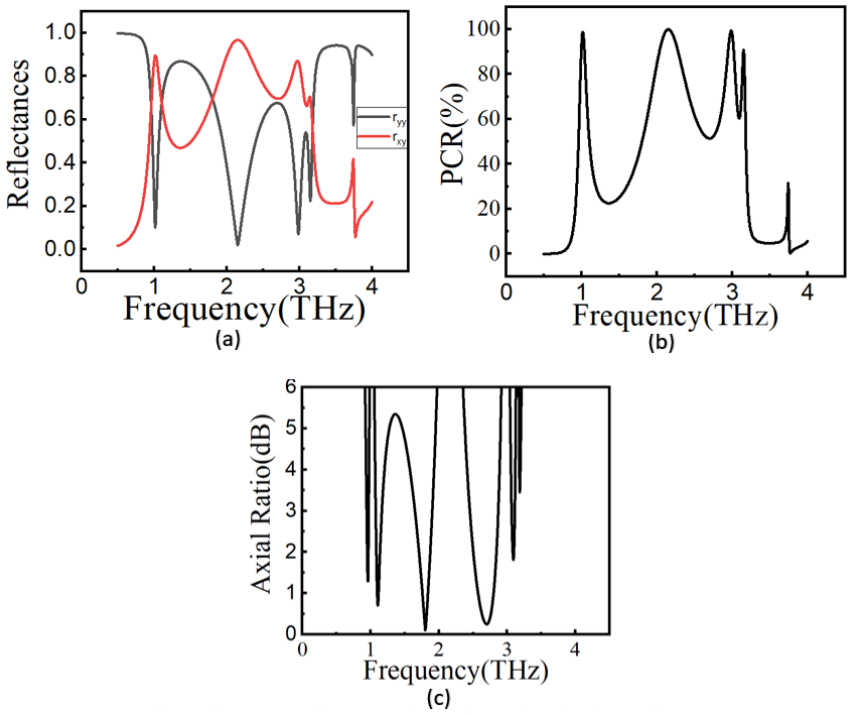


Figure 3.11: Simulated reflectances (a) magnitudes (b)PCR and (c)AR.

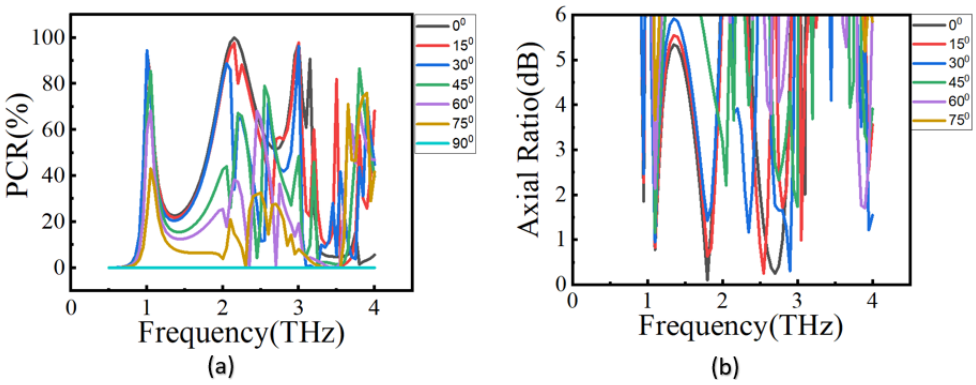


Figure 3.12: Simulated (a)PCR and (b)AR(dB) for different angles.

## 3.6 Square loop PC

The design of the proposed multi-band reflective polarizer consists primarily of the top FSS and the ground, as shown in fig(3.13). Both were separated by a 25µm thin polyamide substrate with relative permittivity $\epsilon_r = 3.5$ and dielectric loss-tangent tan $\delta = 0.02$. A 0.2 µm thin gold layer is used as a metallic film to serve the purpose. The finalized dimensions of the proposed polarization converter are as follows: P =74µm, l =35µm, w =2µm, w1 =1µm, s =2µm, g =2µm, h =25µm, and t =0.2µm. Here, P denotes the unitcell periodicity, l,s,w,g are the different unitcell dimensions fig(3.13), h and t denote the dielectric spacer's thickness, and metallic gold film, respectively.

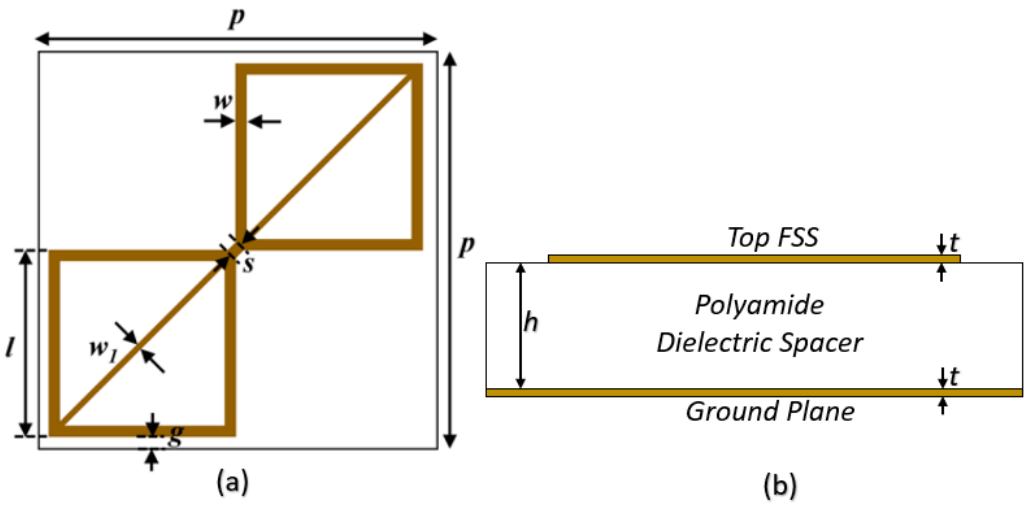


Figure 3.13: (a) Top and (b) side view of the square loop polarizer.

## Performance analysis

The simulated reflectances of the proposed design are depicted in fig(3.14a). From fig(3.14a), it is clear that the magnitude of the co-pol ($r_{yy}$) reaches a minimum at three resonant frequencies, 0.570THz, 1.040THz, and 1.740THz, respectively, while the cross-pol ($r_{xy}$) reaches the maximum at these frequencies. The simulated PCR response of the proposed design is given in fig(3.14b). The PCR is greater than 90% over 0.53-0.56THz, 0.92-1.07THz, and 1.69-1.75THz. In addition to the linear-cross conversion, this design also performs linear-circular polarization conversion in different frequency regions. The simulated Axial Ratio (AR) of the proposed design for y-polarized incidence is depicted in fig(3.14b). The AR is 3 dB over from 0.49-0.50THz, 0.60-0.83THz, 1.16-1.62THz, 1.81-1.85THz, respectively. The simulated phases of co-pol and cross-pol components and relative phases are depicted in fig(3.14d)

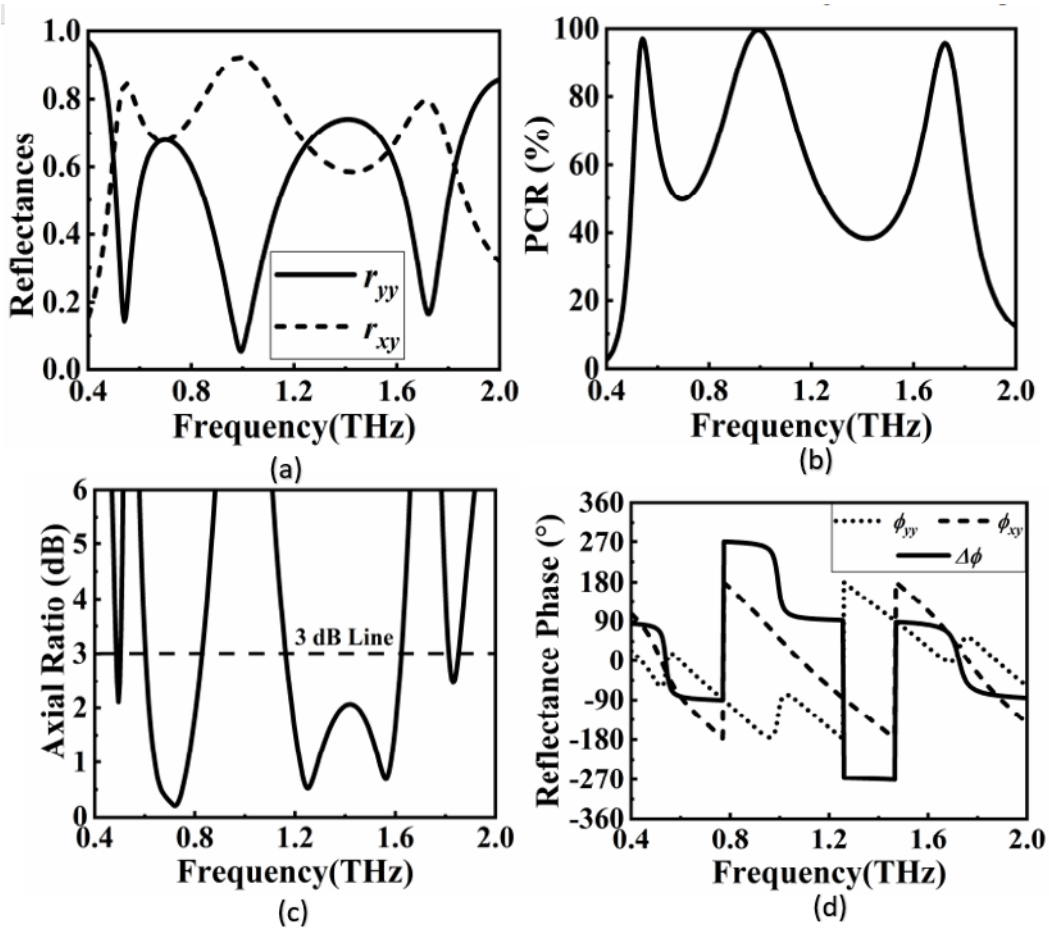


Figure 3.14: Simulated reflectances (a) magnitudes, (b)PCR, (c)AR and (d)phase.

In general, the wave incident on to metasurface won't be in the normal direction

always. Since the surface impedance variation is not the same for Transverse Electric (TE) and Transverse Magnetic (TM) modes, the PCR and AR variations for TE and TM modes at different angles are investigated, and the performance is depicted in fig(3.15). The incident angle is varied from $0^0$ to $60^0$ in steps of $15^0$. From the response, it is clear that the response is stable up to $45^0$ and a slight deviation is observed at $60^0$.

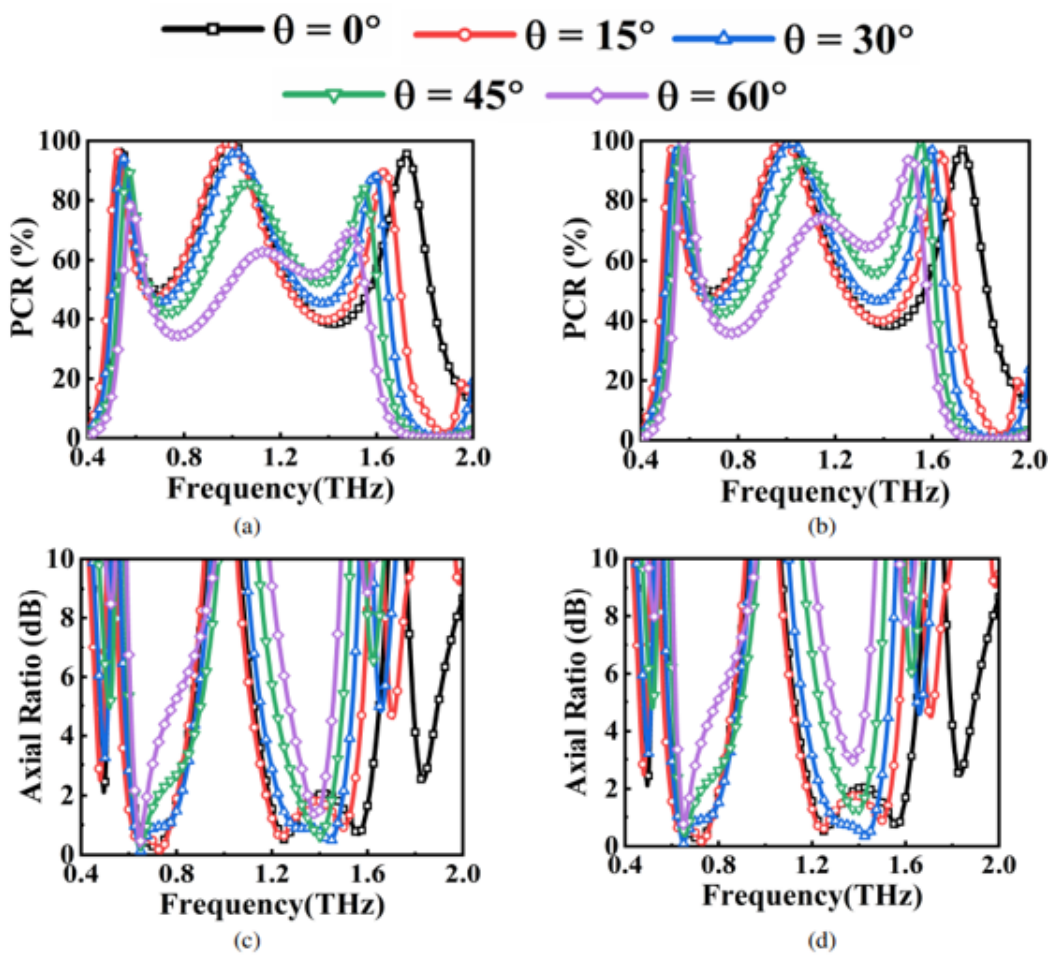


Figure 3.15: Simulated PCR for the (a) TE (b) TM, and AR (dB) for the (c) TE and (d) TM modes for different angles ($\theta$).

## 3.7 Circular loop PC

Schematic of the proposed multiband polarization converter is shown in fig (3.16). The designed structure is made up of three layers, the top FSS, a bottom metallic ground plate and a dielectric substrate separating the two having a height 20µm.

Polyamide with a relative permittivity $\epsilon_r = 3.5$ and dielectric loss-tangent tan $\delta = 0.02$ act as the substrate. The bottom metallic ground plane and top FSS is made of a 0.2um thin gold layer. The final dimensions of the proposed structure are as follows: P = 79µm, r1 =28µm, r2 =25µm, k1 =18µm, k2 =15µm, w =3µm g =2µm, h =20µm and t =0.2µm. Where, P denotes the periodicity of unitcell, r1 and r2 is the inner and outer radius of the cylinder in the centre. The inner and outer radius of the two small cylinders is k1 and k2(see fig(3.16a)), h and t denote the dielectric spacer's thickness and metallic gold film, respectively.

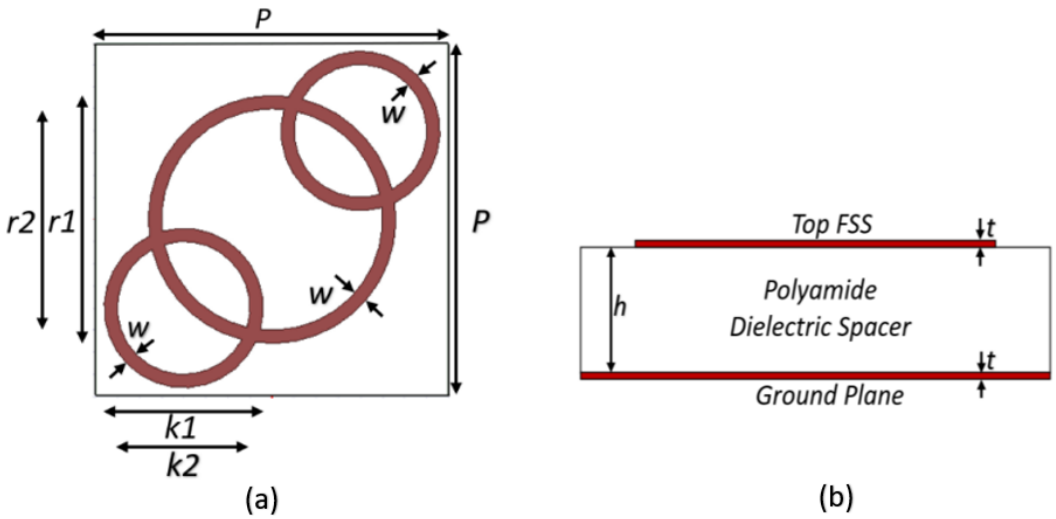


Figure 3.16: (a) Top and (b) side view of the circular loop polarizer.

## Performance analysis

The reflectance graph of the proposed structure is rendered in fig (3.17a). From fig(3.17a) its clear that the co-pol ($r_{yy}$) is minimum at the three resonant frequencies 0.68THz, 1.03THz and 1.77THz, while the cross-pol ($r_{xy}$)is maximum at these frequencies. To assess the linear-cross performance of the unitcell, it's PCR is calculated. The PCR of the simulated design is shown in fig(3.17b). The PCR is above 90% for the frequencies 0.62-0.65THz, 0.98-1.10THz and 1.74-1.80THz. Besides Linear to cross conversion, it can also perform linear to circular conversion at different frequencies. The circular polarization efficiency is calculated from the Axial Ratio. The simulated AR is 3 dB over the ranges 0.58-0.59THz, 0.69-0.90THz, 1.18-1.67THz and

1.87-1.90THz, as shown in fig(3.17c). The simulated phases of co-pol and cross-pol components and relative phases are depicted in fig(3.17d).

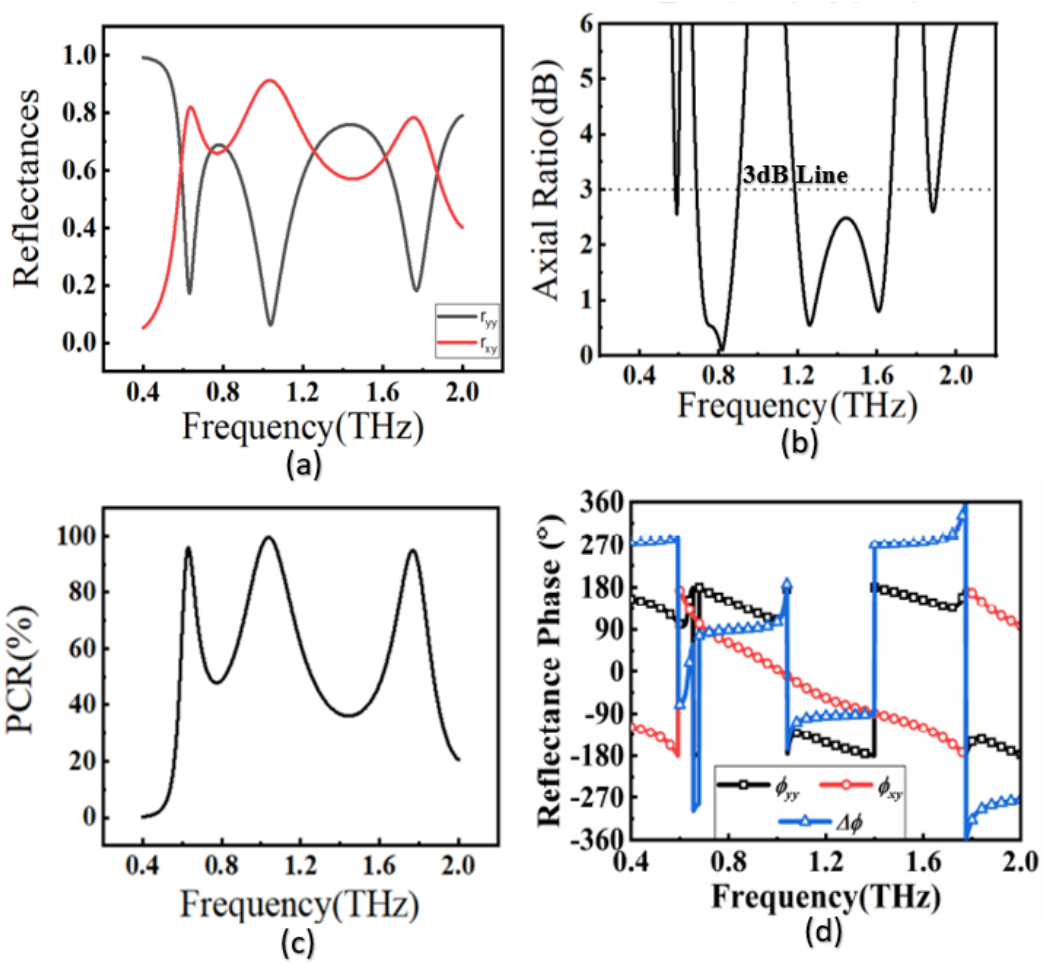


Figure 3.17: Simulated reflectances (a) magnitudes, (b)PCR, (c)AR and (d)Phase.

The wave incidence on the metasurface will typically not always be in the normal direction. Since the surface impedance variation for Transverse Electric (TE) and Transverse Magnetic (TM) modes differs, it makes compulsory to investigate the deviation of the PCR and AR performance regarding incident angles. The performance is shown in fig(3.18) for the PCR and AR variations for TE and TM modes at various angles in 15° steps, 0° to 60°. The response makes it evident that the response is stable up to a $45^0$ angle and that a small variation was seen at $60^0$.

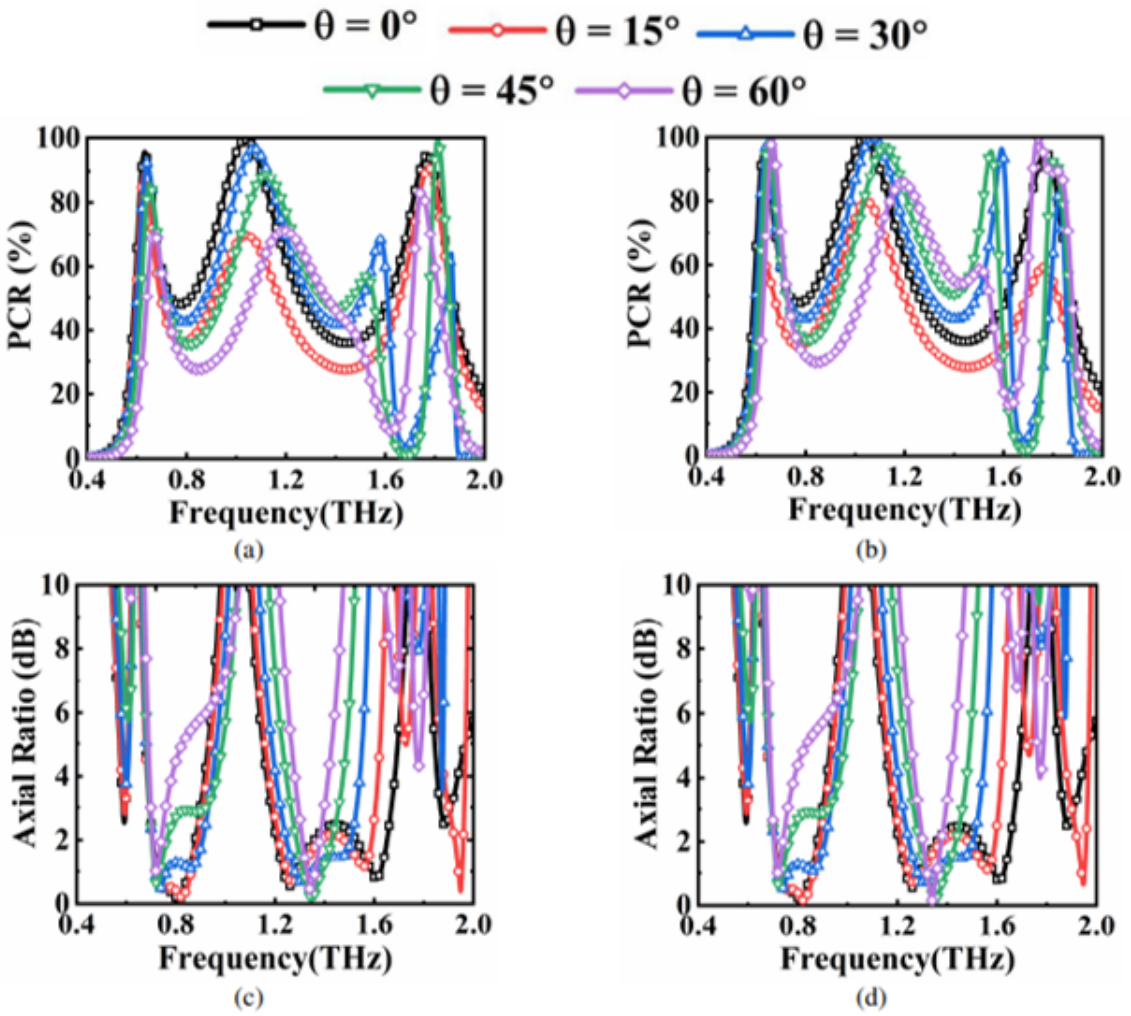


Figure 3.18: Simulated PCR for the (a) TE (b) TM, and AR (dB) for the (c) TE and (d) TM modes for different angles ($\theta$).

# Chapter 4

# Results and discussion

Silicon dioxide and polyamide were used as substrate in the designed structures. The polarization converters built with polyamide has better polarization conversion efficiency than the one made with $SiO_2$. The square loop FSS and circular loop FSS has high performance in the THz realm. In addition, polyamide has excellent heat resistance capacity, high durability and is easy to integrate with gold films.

## 4.1 Square loop PC

It is also necessary to estimate how much energy the substrate absorbs during multiple reflections of EM waves between FSS and the ground. Hence, the term Energy Conversion Ratio,

$$ECR = r_{xy}^2 + r_{yy}^2 \tag{4.1}$$

is calculated, as depicted in fig(4.1). Almost 90% of the incident energy is reflected, and the remaining energy dissipation is considered substrate and metallic losses. It is noteworthy to mention that there are three dips in the curve representing the resonance nature of the surface plasmons of these structures.

### 4.1.1 Surface current distribution

When an EM incident on the metasurface, the symmetric and asymmetric coupling of electric and magnetic fields induces surface currents in the metallic portion of the unitcell. This current linkage induces plasmonic resonance and would be re-

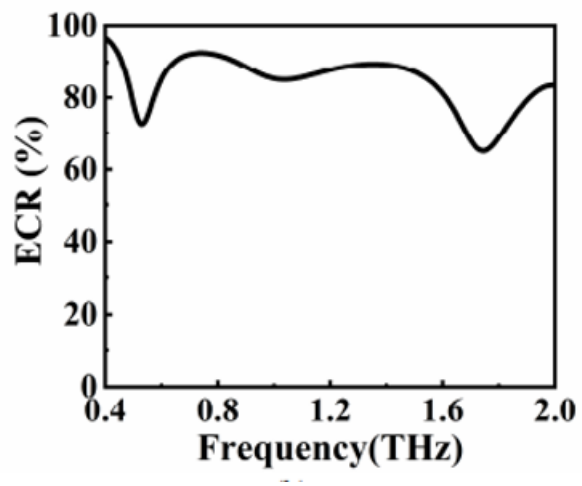


Figure 4.1: ECR performance of the square loop polarizer.

sponsible for the polarization conversion. In order to get the physical insight into the multi-polarization conversion involved, the surface current distribution patterns are investigated at resonant frequencies 0.570THz, 1.040THz and 1.740THz, as depicted in fig(4.2). At 0.570THz, it seems clear that the surface currents induced in the top FSS are out of phase by $180^0$ with the current induced in the ground. These anti-parallel currents resemble magnetic dipoles resulting in magnetic or dielectric resonance [1]. A similar anti-parallel current behavior is observed at frequency 1.040THz (magnetic resonance). But at 1.740THz, the surface currents are in a phase that resembles electric dipole resonance. The analysis shows that electric and magnetic resonance is responsible for the wideband polarization conversion. In addition, the ground surface current patterns are investigated at three more resonant frequencies, 0.760THz, 1.350THz, and 1.510THz having Axial Ratio 0.464dB, 0.291dB and 0.290dB, respectively, as shown in fig(4.3). The main motive for this analysis is to demonstrate the sense of the circular rotation, whether it is Right or Left-handed. At 0.760THz, from the surface currents at different incident EM phase t = $0^0$ to $270^0$, it is clear that the reflected wave would be Right Circular Polarized. On the other hand, the next two frequencies, 1.350THz and 1.510THz, clearly demonstrate that the reflected wave would be Left-hand Circularly polarized.

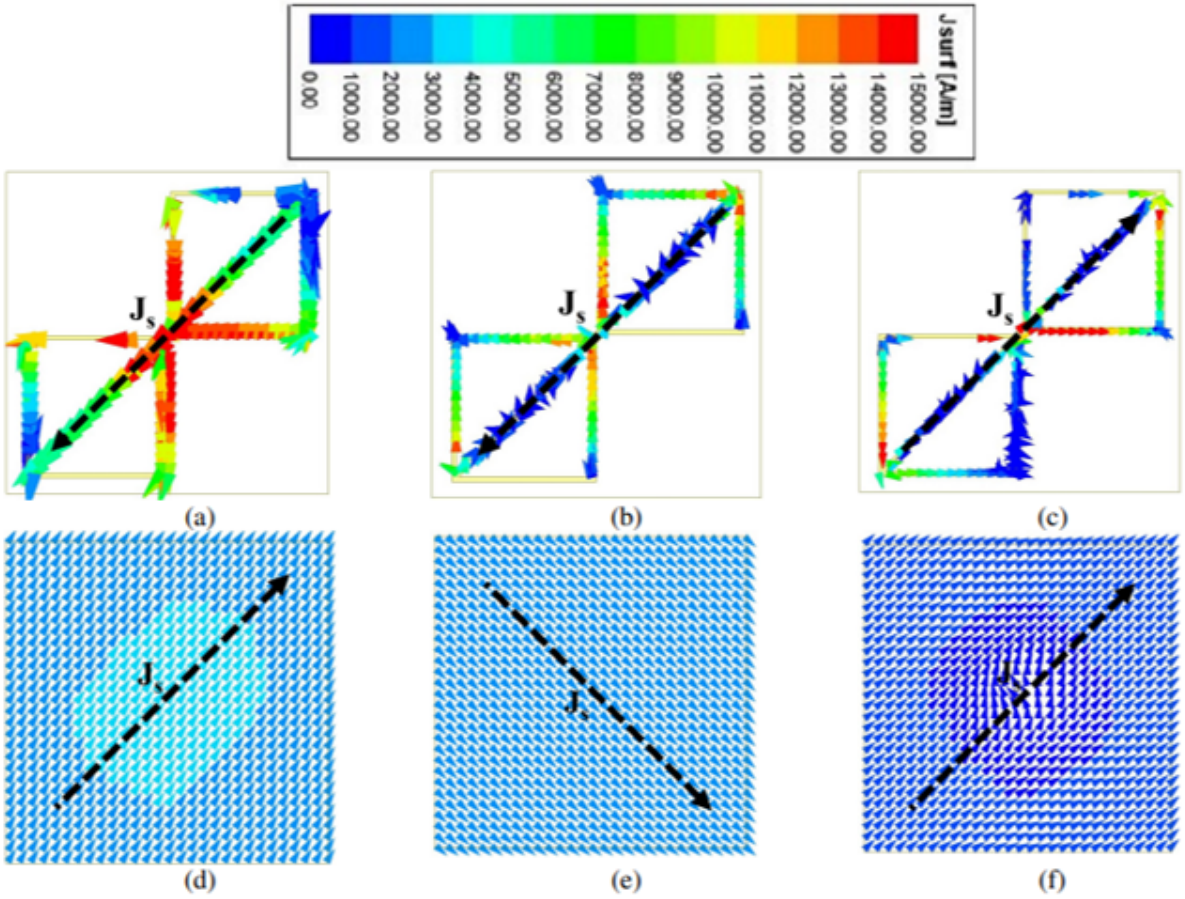


Figure 4.2: Surface current profile of top FSS at (a) 0.570 THz, (b) 1.040 THz, (c) 1.740 THz, and ground at (d) 0.570 THz, (e) 1.040 THz, (f) 1.740 THz.

### 4.1.2 Analysis using Transfer Matrix Method (TMM)

To understand the working mechanism of polarization conversion in detail, two axes, u- and v-are defined at $45^0$ offset concerning xy-axes [28], as shown in fig(4.4). Since the unitcell asymmetry along x/y-axes, the incident electric field ($\overrightarrow{E_l}$) of the wave travelling along +z direction, can be written as orthogonal sum of field components along u- and v-components, respectively,

$$(\overrightarrow{E_l}) = (E_i^u \tilde{u} + E_i^v \tilde{v}) e^{jkz} \tag{4.2}$$

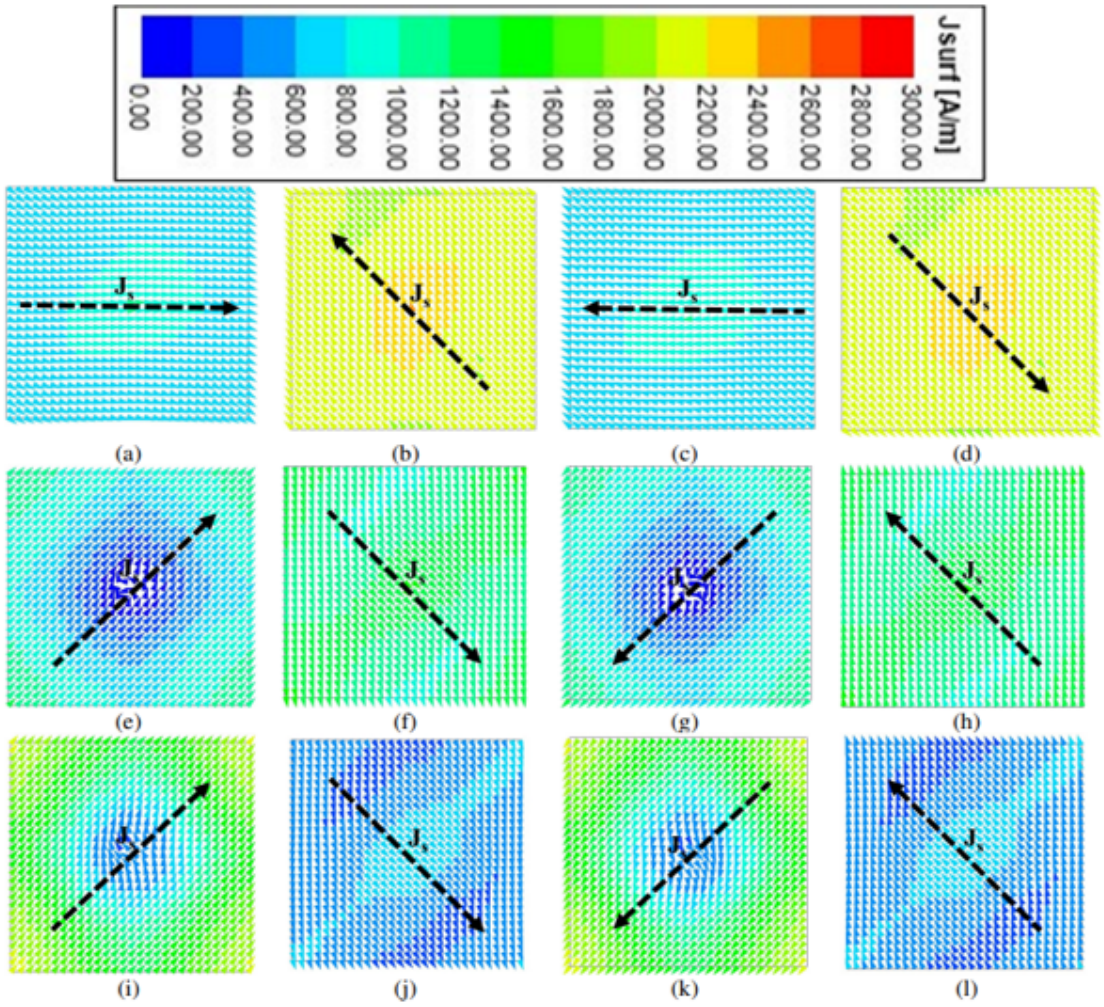


Figure 4.3: Surface current profile of the ground plane at 0.76 THz for incident wave phase ($\omega t$) (a) $0^0$ , (b) $90^0$ , (c) $180^0$ , (d) $270^0$ . At 1.35 THz for incident wave phase ($\omega t$) (e) $0^0$ , (f) $90^0$ , (g) $180^0$ , (h) $270^0$ and at 1.51 THz for incident wave phase ($\omega t$) (i) $0^0$ , (j) $90^0$ , (k) $180^0$ , (l) $270^0$.

The reflected electric field component can be obtained from the Transfer Matrix Method (TMM), as in [1]

$$\begin{bmatrix} E_r^u \\ E_r^v \end{bmatrix} = \begin{bmatrix} r_{uu} & r_{uv} \\ r_{vu} & r_{vv} \end{bmatrix} \begin{bmatrix} E_i^u \\ E_i^v \end{bmatrix} \tag{4.3}$$

Due to the structure symmetry along u- and v-axes, the cross-pol components $r_{uv}$ and $r_{vu}$ are almost negligible, and the reflected electric field component would be summarized as

$$\overrightarrow{E_r} = (r_{uu}E_i^u\tilde{u} + r_{vv}E_i^v\tilde{v})e^{jkz} \tag{4.4}$$

Here, $r_{uu}$ and $r_{vv}$ are the complex co-pol reflection coefficients of u-, v-incidences,

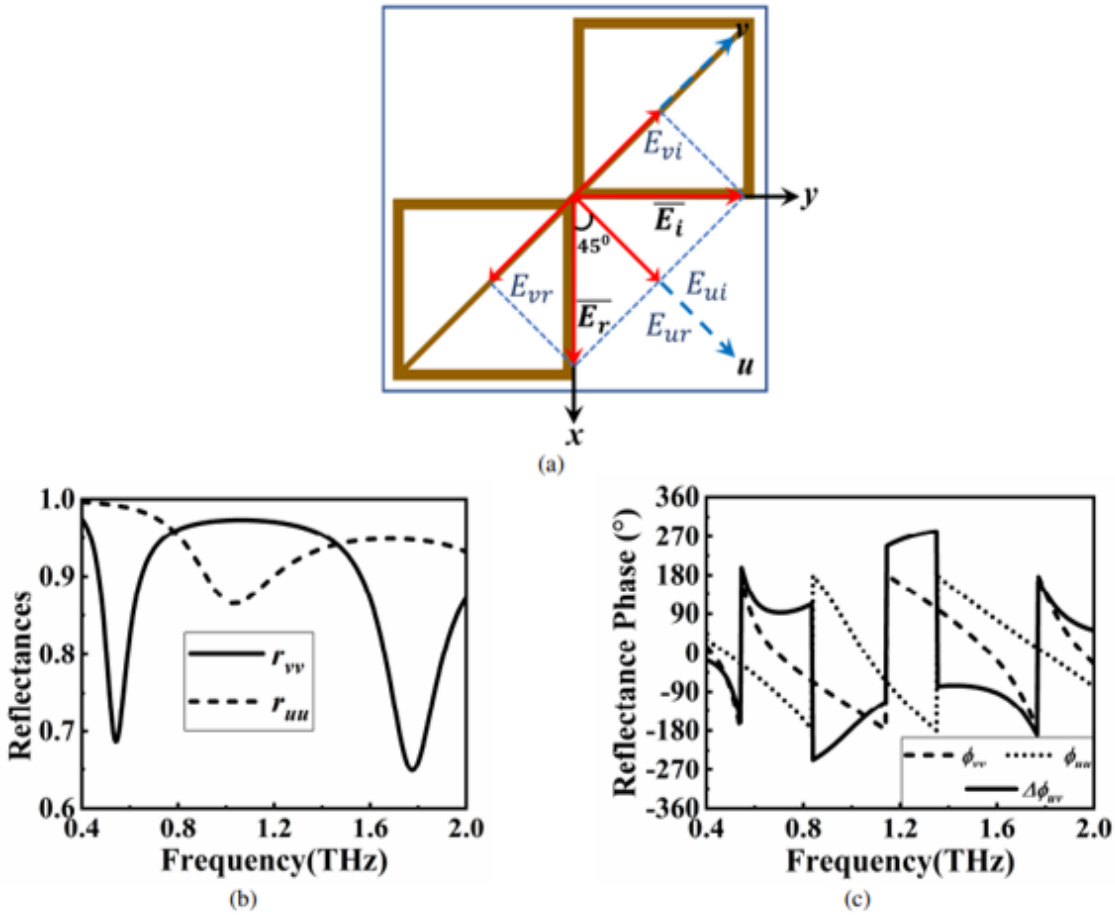


Figure 4.4: (a) Schematic diagram of the proposed unitcell with uv-axes. Simulated reflectance (b) magnitudes, and (c) phases of $r_{uu}$ and $r_{vv}$.

respectively. These components' simulated magnitudes and phases are depicted in fig (4.4b) and fig(4.4c), respectively. Co-pol components' magnitudes are almost uniform with small dips due to resonant phenomena at 0.545THz, 1.035THz, and 1.775THz. If the losses due to the dielectric substrate are neglected, then the reflected fields would be $r_{uu} = e^{j\phi_u}$, $r_{vv} = e^{j\phi_v}$ and $\Delta\phi_{uv} = \phi_u - \phi_v$. Here, $\Delta\phi_{uv}$ is the relative phase between $r_{uu}$ and $r_{vv}$. Due to the asymmetry of the proposed structure, a relative phase is generated. In order to convert polarization from y to x, a stable relative phase ($\Delta\phi_{uv}$) of $\pm\pi$ would be necessary (see fig (4.4c)).

If $\Delta\phi_{uv}$=$+\pi$ means $\phi_u = \pi$, and $\phi_v = 0$ results $r_{uu}$=-1, and $r_{vv}$=+1. Then, the reflected field component would be $\overrightarrow{E_r} = (-E_i^u\tilde{u} + E_i^v\tilde{v})e^{-jkz}$ is along the negative x-direction. Next, for the case $\Delta\phi_{uv} = -\pi$ means $\phi_u = 0$ and $\phi_v = \pi$ results $r_{uu}$=+1, and $r_{vv}$=-1. The reflected field component now will be $\overrightarrow{E_r} = (+E_i^u\tilde{u} - E_i^v\tilde{v})e^{-jkz}$ is

along the positive x-direction since the structure is dual-polarized if the x- polarized wave incident on the metasurface is converted into a y-polarized one.

For the linear-circular conversion, the relative phase $\Delta\phi_{uv}$ will be $\pm\frac{\pi}{2}$. For a y-polarized incidence, If $\Delta\phi_{uv} = \frac{\pi}{2}$, means $\phi_u = -\frac{\pi}{2}$ and $\phi_v = +\pi$ results $r_{uu}$=-j and $r_{vv}$=-1. The reflected field would be $\overrightarrow{E_r} = (-jE_i^u\tilde{u} - E_i^v\tilde{v})e^{-jkz}$ will result in the linearly y-polarized incident wave to Left Hand Circular Polarization Conversion (LHCP). On the other hand, if $\Delta\phi_{uv} = -\frac{\pi}{2}$ means $\phi_u = -\frac{\pi}{2}$, and $\phi_v = -\pi$. In this case, the reflected field component $\overrightarrow{E_r} = (+jE_i^u\tilde{u} - E_i^v\tilde{v})e^{-jkz}$ represent the Right Hand Circularly Polarized wave during reflection. It is also noteworthy that the sense of circular rotation would be interchanged if the y-incidence is replaced by the x-polarized.

## 4.2 Circular loop PC

The amount of energy getting dissipated in the substrate during the multiple reflection between the FSS and ground is estimated by Energy Conversion Ratio (ECR),eq(4.1),fig(4.5).It is observed that nearly 90% of the incident energy is reflected, and the remaining energy is thought to be lost by the substrate (as dielectric losses) and the metals (as ohmic or conductor losses). It is important to note that the ECR curve has three dips, which stand for the resonance properties of the surface plasmons of these structures.

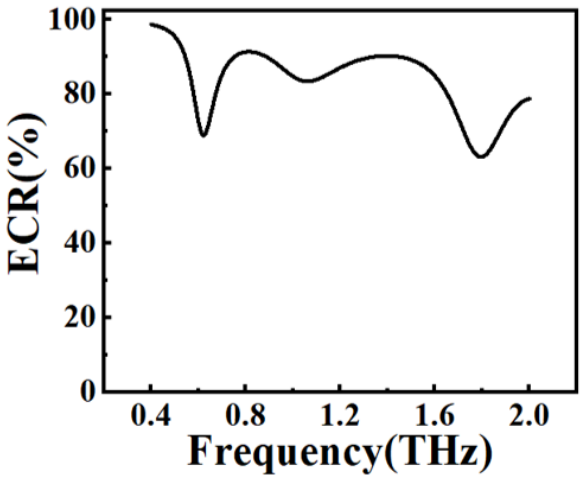


Figure 4.5: ECR performance of the circular loop polarizer.

### 4.2.1 Surface current distribution

Surface current patterns are investigated to find the physical phenomena behind polarization conversion. Surface current is induced in the metallic portion of unit cell due to symmetric and asymmetric coupling of electric and magnetic fields. In turn it induces plasmonic resonance which is responsible for the polarization conversion. The surface current distribution patterns are investigated at resonant frequencies 0.68THz, 1.03THz, and 1.77 THz, as depicted in fig(4.6). At 0.68THz the surface currents induced in the top FSS are out of phase by $180^0$ with the current induced in the ground. These anti-parallel currents resemble magnetic dipoles resulting in magnetic or dielectric resonance. Similarly at 1.03THz also antiparallel current behaviour is observed. But at 1.77THz, the surface currents are in a phase that resembles electric

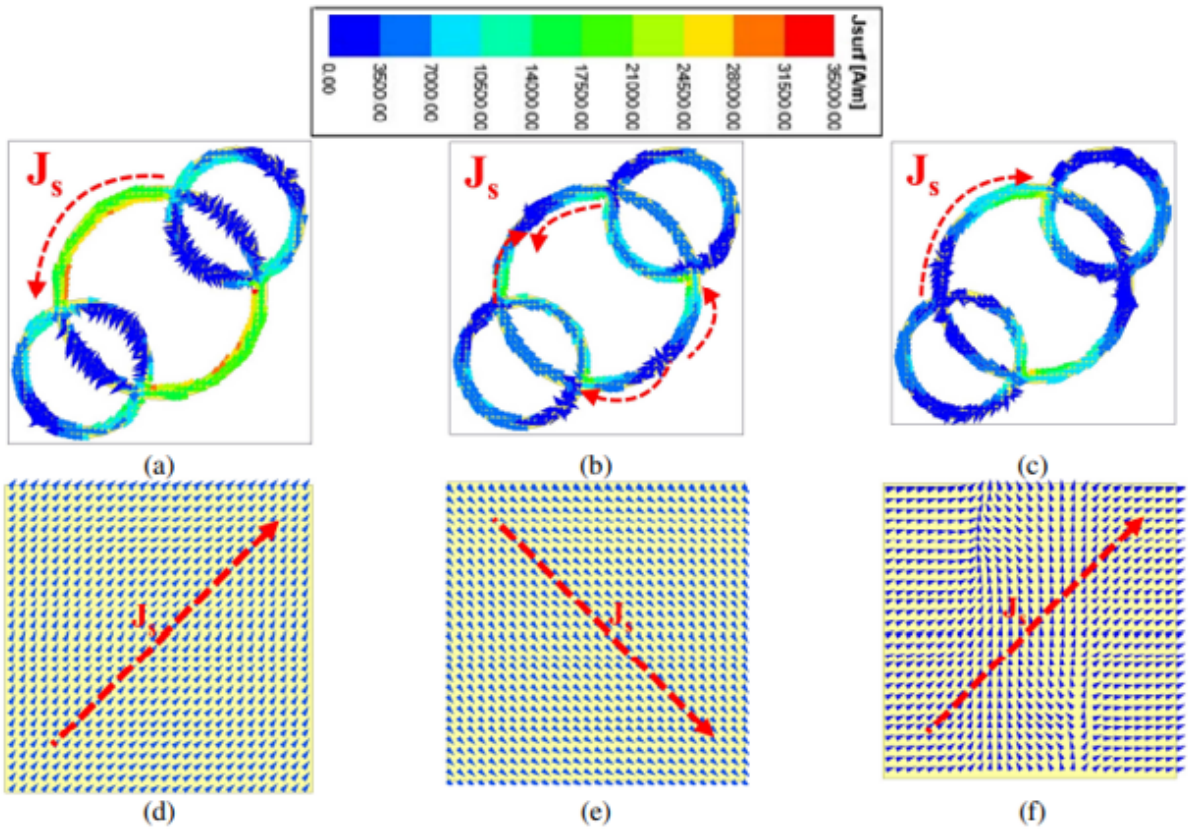


Figure 4.6: Surface current profile of top FSS at (a) 0.68THz, (b) 1.03THz, (c) 1.77THz, and ground at (d) 0.68THz, (e) 1.03THz, (f) 1.77THz.

dipole resonance. In addition, the ground surface currents patterns are investigated at three more resonant frequencies, 0.75THz, 1.35THz, 1.55THz and 1.88THz as shown in fig(4.7). The main motive for this analysis is to demonstrate the sense of the circular rotation, whether it is Right or Left-handed. At 0.75THz, it is observed that the surface currents at different incident EM phase t = $0^0$ to $270^0$, it is clear that the reflected wave would be Right Circular Polarized. On the other hand, the next two frequencies, 1.35THz and 1.55 THz clearly demonstrate that the reflected wave would be Left-hand Circularly polarized.

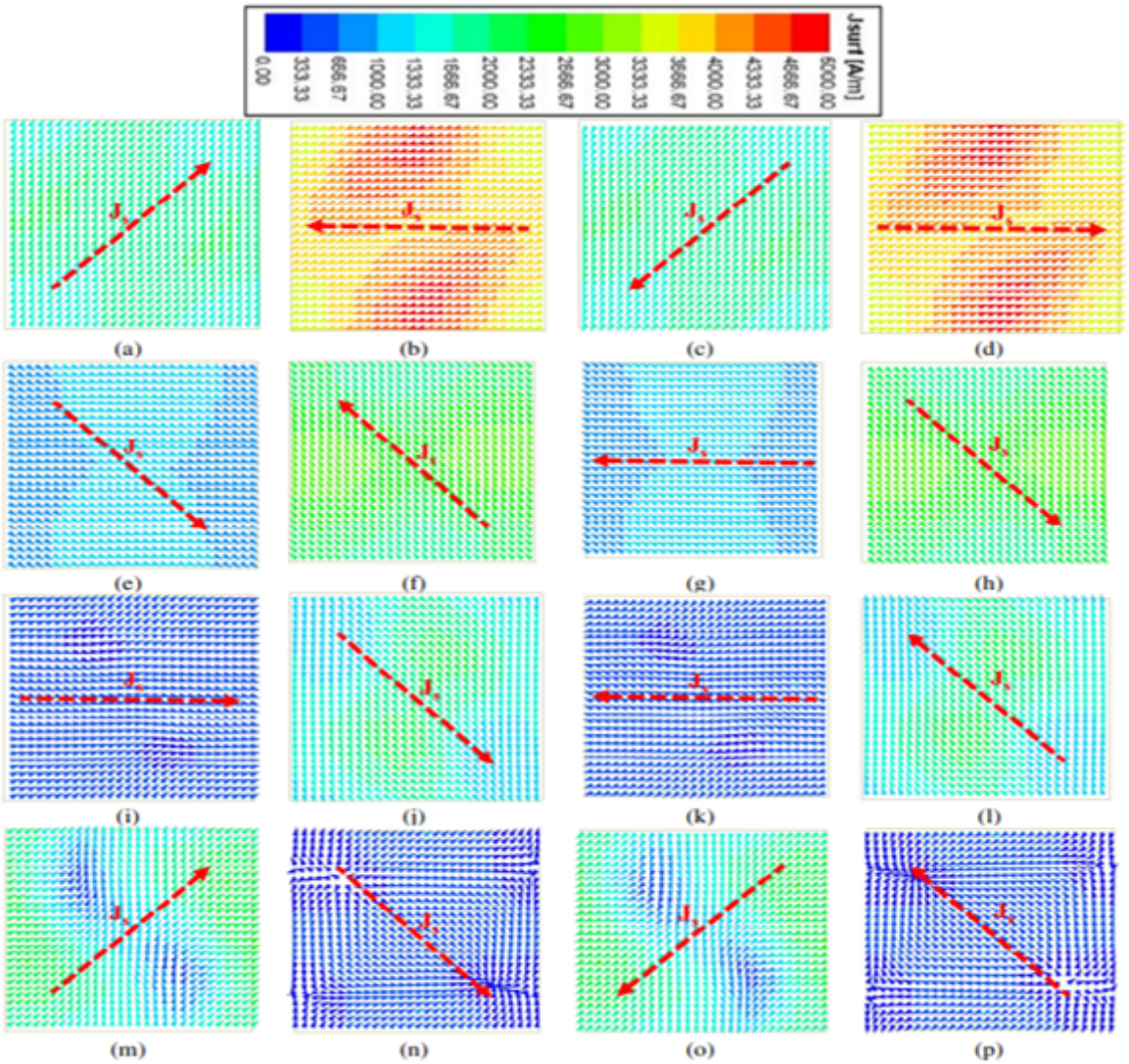


Figure 4.7: Surface current profile of the ground plane at 0.529 THz for incident wave phase ($\omega t$) (a) $0^0$ , (b) $90^0$ , (c) $180^0$ , (d) $270^0$ . At 0.812 THz for incident wave phase ($\omega t$) (e) $0^0$ , (f) $90^0$ , (g) $180^0$ , (h) $270^0$ . At 1.262 THz for incident wave phase ($\omega t$) (i)$0^0$ , (j) $90^0$ , (k) $180^0$ , (l) $270^0$ , and at 1.610 THz for incident wave phase ($\omega t$) (m) $0^0$ , (n) $90^0$ , (o) $180^0$ , (p) $270^0$ .

### 4.2.2 Analysis using Transfer Matrix Method (TMM)

To comprehend the working mechanism behind a polarization conversion, two orthogonal axes, u-and v-, are specified at 45° counter clockwise to the x-y axes as shown in fig (4.8). The incident electric field ($\overrightarrow{(E_l)}$) of the wave travelling along +z direction, can be written as orthogonal sum of field components along u- and v-components, where $E_i^u$ and $E_i^v$ are the components along u- and v-axes.

$$\overrightarrow{(E_l)} = (E_i^u \tilde{u} + E_i^v \tilde{v}) e^{jkz} \tag{4.5}$$

From the TMM technique [1], the reflected field components can be written as

$$\begin{bmatrix} E_r^u \\ E_r^v \end{bmatrix} = \begin{bmatrix} r_{uu} & r_{uv} \\ r_{vu} & r_{vv} \end{bmatrix} \begin{bmatrix} E_i^u \\ E_i^v \end{bmatrix} \tag{4.6}$$

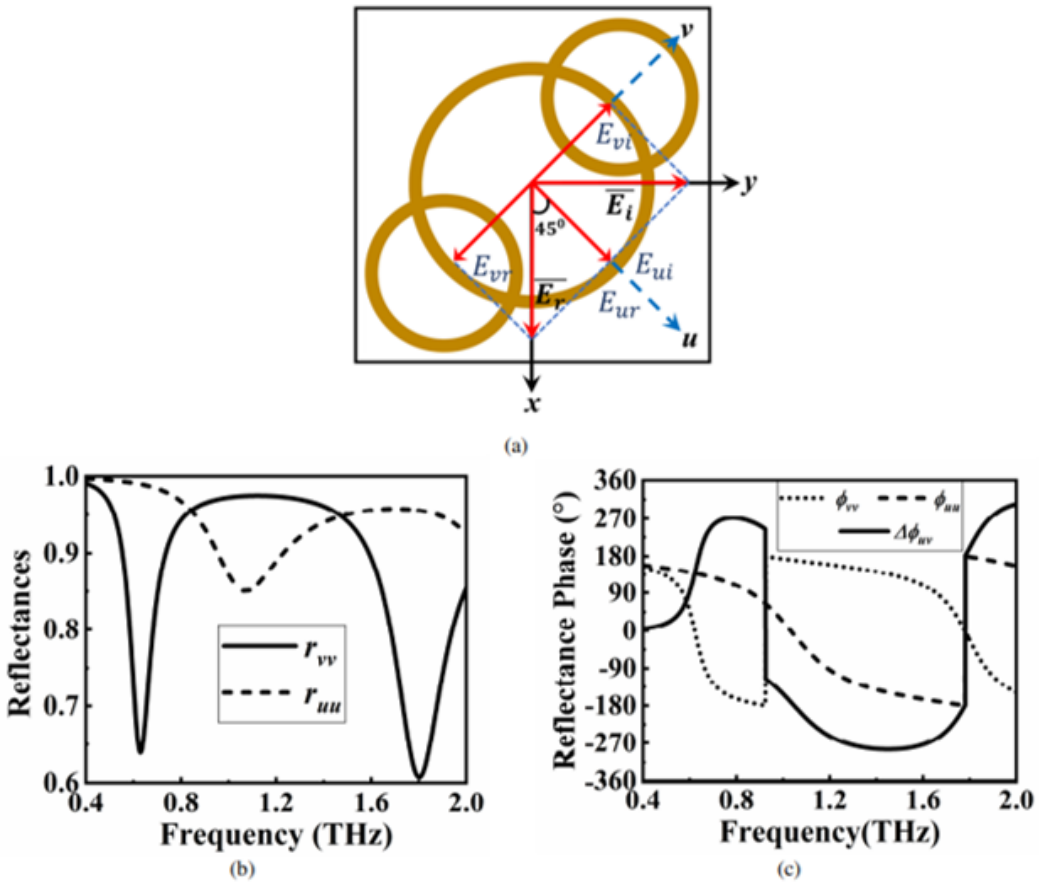


Figure 4.8: (a) Schematic diagram of the proposed unitcell with uv-axes. Simulated reflectance (b) magnitudes, and (c) phases of $r_{uu}$ and $r_{vv}$.

The cross-pol components $r_{uv}$ and $r_{vu}$are essentially insignificant due to the structural symmetry along u- and v-axes, and the reflected electric field component would be defined as $\overrightarrow{E_r} = (r_{uu}E_i^u\tilde{u} + r_{vv}E_i^v\tilde{v})e^{-jkz}$. Here, $r_{uu}$ and $r_{vv}$ are co-pol complex reflection coefficients for u- and v-incidences. Fig(4.8b) and (4.8c) show the simulated magnitudes and phases for uv-excitations. The magnitudes of the co-pol components are nearly uniform, with only minor dips caused by resonant phenomena at 0.630, 1.080 and 1.802 THz. If the losses resulting from the dielectric substrate are disregarded, then the reflected fields would be $r_{uu} = e^{j\phi_u}$, $r_{vv} = e^{j\phi_v}$ and $\Delta\phi_{uv} = \phi_u - \phi_v$. Note that $\Delta\phi_{uv}$ is the relative phase between phase components between $r_{uu}$ and $r_{vv}$. The relative phase is produced as a result of the proposed structure's asymmetries, and the stable relative phase ($\Delta\phi_{uv}$ ) of $\pm$ would be required to change the polarization from y to x.

If $\Delta\phi_{uv}$=$+\pi$ means $\phi_u = \pi$, and $\phi_v = 0$ results $r_{uu}$=-1, and $r_{vv}$=+1. Then, the reflected field component would be $\overrightarrow{E_r} = (-E_i^u\tilde{u} + E_i^v\tilde{v})e^{-jkz}$ is along the negative x-direction. Next, for the case $\Delta\phi_{uv} = -\pi$ means $\phi_u = 0$ and $\phi_v = \pi$ results $r_{uu}$=+1, and $r_{vv}$=-1. The reflected field component now will be $\overrightarrow{E_r} = (+E_i^u\tilde{u} - E_i^v\tilde{v})e^{-jkz}$ is along the positive x-direction since the structure is dual-polarized if the x- polarized wave incident on the metasurface is converted into a y-polarized one.

For the linear-circular conversion, the relative phase $\Delta\phi_{uv}$ will be $\pm\frac{\pi}{2}$. For a y-polarized incidence, If $\Delta\phi_{uv} = \frac{\pi}{2}$, means $\phi_u = -\frac{\pi}{2}$ and $\phi_v = +\pi$ results $r_{uu}$=-j and $r_{vv}$=-1. The reflected field would be $\overrightarrow{E_r} = (-jE_i^u\tilde{u} - E_i^v\tilde{v})e^{-jkz}$ will result in the linearly y-polarized incident wave to Left Hand Circular Polarization Conversion (LHCP). On the other hand, if $\Delta\phi_{uv} = -\frac{\pi}{2}$ means $\phi_u = -\frac{\pi}{2}$, and $\phi_v = -\pi$. In this case, the reflected field component $\overrightarrow{E_r} = (+jE_i^u\tilde{u} - E_i^v\tilde{v})e^{-jkz}$ represent the Right Hand Circularly Polarized wave during reflection.

## 4.3 Comparison of designs

Table 4.1: Comparison of different unit cells

| Designed unit cells | 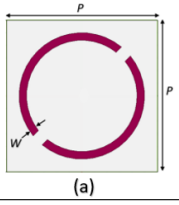 (a) | 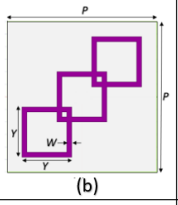 (b) | 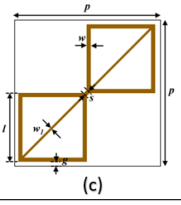 (c) | 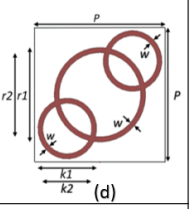 (d) |
|---|---|---|---|---|
| Substrate | $SiO_2$ | $SiO_2$ | Polyamide | Polyamide |
| PCR is above 90% for frequencies(THz) | 1.12-1.17, 2.01-2.17 | 1.03-1.07,2.10-2.35, 3.05-3.20 | 0.53-0.56, 0.92-1.07, 1.69-1.75 | 0.62-0.65, 0.98-1.10, 1.74-1.80 |
| Axial Ratio is below 3dB for frequencies(THz) | 1.06-1.10, 1.22-1.34, 1.68-1.91, 2.24-2.37 | 0.97-1.01, 1.11-1.20, 1.70-1.96, 2.53-2.97 | 0.49-0.50, 0.60-0.83, 1.16-1.62 | 0.58-0.59, 0.69-0.90, 1.18-1.67,1.87-1.90 |
| Angular stability(degree) | NA | NA | 45 | 45 |

The split ring PC shown in table 4.1(a) has the ability to convert linear polarized wave to cross at frequency bands 1.12-1.17THz, 2.01-2.17THz with a PCR above 90% and linear to cross with an axial ratio below 3dB for frequency bands 1.06-1.10THz, 1.22-1.34THz, 1.68-1.91THz, 2.24-2.37THz. But the main drawback observed in this structure is its angular instabilty. Three square loop PC depicted in table 4.1(b) was able to convert linear polarised wave to cross with PCR above 90% for frequency bands 1.03-1.07THz, 2.10-2.35THz, 3.05-3.20THz . The axial ratio was below 3dB at frequency bands 0.97-1.01THz, 1.11-1.20THz, 1.70-1.96THz, 2.53-2.97THz. The snag with this design is its angular stability. The square loop PC given in table 4.1(C) can convert arriving frequencies to linear to cross in 0.53-0.56THz, 0.92-1.07THz, 1.69-1.75THz PCR above 90%. Linear to circular polarization occur at frequencies 0.49-0.50THz, 0.60-0.83THz, 1.16-1.62THz where axial ratio is below 3dB. Additionally, the structure is angular stable for incidence upto $45^0$. The circular loop PC in table 4.1(d) act as a linear to cross polarizer in frequencies 0.62-0.65THz, 0.98-1.10THz, 1.74-1.80THz. Axial ratio is below 3dB for frequencies 0.58-0.59THz, 0.69-0.90Thz, 1.18-1.67THz, 1.87-1.90THz where linear to circular polarization conversion occur. Furthermore, the design is angular stable upto $45^0$ of incidence.

From the above comparison it's clear that polarization converters have PCR above 90% and AR below 3dB. However, the polarization converters designed with $S_iO_2$ as

substrate(Split ring,three square loop) is not angular stable. The polarization converters with polyamide as substrate is angular stable upto $45^0$ of incidence. In a nut shell it can be said that PC made with polyamide has better performance in the THz region than the one made with $S_iO_2$ .

Table 4.2: Comparison of the proposed designs with the other recently reported polarizers.

| Ref | Periodicity (in $\lambda_L^2$) | Thickness (in $\lambda_L$) | Volume (in $\lambda_L^3$/1000) | Polarization Conversion | Freq range (THz) | Angular stability |
|---|---|---|---|---|---|---|
| [40] | 0.324×0.649 | 0.055 | 11.679 | Linear-Circular | 0.83-1.03 | NA |
| [41] | 0.380x0.380 | 0.109 | 15.727 | Linear-Circular | 0.94-1.38 | NA |
| [37] | 0.185x0.185 | 0.068 | 2.327 | Linear-Cross | 7.2-11.12 | 30° |
| | | | | | 15.2-15.7 | |
| | | | | Linear-Circular | 5.77-6.38 | 45° |
| | | | | | 12.4-14.0 | |
| Square loop PC | **0.121×0.121** | **0.041** | **0.600** | **Linear-Circular** | **0.49-0.50** | **45°** |
| | | | | | **0.60-0.83** | |
| | | | | | **1.16-1.62** | |
| | | | | **Linear-Cross** | **0.53-0.56** | |
| | | | | | **0.92-1.07** | |
| | | | | | **1.69-1.75** | |
| Circular loop PC | **0.153×0.153** | **0.039** | **0.912** | **Linear-Cross** | **0.62-0.65** | **45°** |
| | | | | | **0.98-1.10** | |
| | | | | | **1.74-1.80** | |
| | | | | **Linear-Circular** | **0.58-0.59** | |
| | | | | | **0.69-0.90** | |
| | | | | | **1.18-1.67** | |
| | | | | | **1.87-1.90** | |

# Chapter 5

# Conclusion

There are many polarization converters that works in the GHz region. The GHz bands are already crowded so there is a need to focus more on the THz bands for future developments. The afore discussed results indicate that the proposed square loop PC and ring loop PC can perform both the LX and LC kinds of conversion in the THz realm. The x polarized wave is converted into its cross component with a PCR above 90% in the two structures. They also exhibits the linear to circular polarisation conversion in multiple frequency bands with an axial ratio below 3dB. Nevertheless, the proposed structures exhibits fairly good angular stability in the polarization conversion operation. This work is complete and useful for fabricating in THz regime. Thus, having great potentials in many EM applications that include antenna engineering, photonic communications and other THz applications.

# REFERENCES

[1] M. A. Shukoor, S. Dey, and S. K. Koul, "Broadband Chiral-type Linear to Linear Reflecting Polarizer With Minimal Bandwidth Reduction at Higher Oblique Angles for Satellite Applications," IEEE Trans. Antennas Propag., pp. 1–1, 2022.

[2] J. F. Federici, Brian Schulkin, Feng Huang, Dale Gary, Robert Barat, Filipe Oliveira and David Zimdars., "THz imaging and sensing for security applications—explosives, weapons and drugs," Semicond. Sci. Technol., vol. 20, no. 7, p. S266, Jun. 2005.

[3] R. Ivaškevičiūtė-Povilauskienė, Linas Minkevičius, Domas Jokubauskis, Andrzej Urbanowicz, Simonas Indrišiūnas, and Gintaras Valušis., "Flexible materials for terahertz optics: advantages of graphite-based structures," Opt. Mater. Express, Vol. 9, Issue 11, pp. 4438-4446, vol. 9, no. 11, pp. 4438–4446, Nov. 2019.

[4] E. Czerwińska, J. A. Monsoriu, M. Szustakowski, P. Zagrajek, V. Ferrando, and W. D. Furlan, "3D printed diffractive terahertz lenses," Opt. Lett. Vol. 41, Issue 8, pp. 1748- 1751, vol. 41, no. 8, pp. 1748–1751, Apr. 2016.

[5] J. Liu, J. Dai, S. L. Chin, and X. C. Zhang, "Broadband terahertz wave remote sensing using coherent manipulation of fluorescence from asymmetrically ionized gases," Nat. Photonics 2010 49, vol. 4, no. 9, pp. 627–631, Jul. 2010.

[6] J. J. Lee, F. T. Schmitt, R. G. Moore, I. M. Vishik, Y. Ma, and Z. X. Shen, "Intrinsic ultrathin topological insulators grown via molecular beam epitaxy characterized by insitu angle resolved photoemission spectroscopy," Appl. Phys. Lett., vol. 101, no. 1, p. 013118, Jul. 2012.

[7] F. Monticone and A. Alù, "Metamaterials and plasmonics: From nanoparticles to nanoantenna arrays, metasurfaces, and metamaterials," Chinese Phys. B, vol. 23, no. 4, p. 047809, Mar. 2014.

[8] W. T. Chen, Kuang-Yu Yang, Chih-Ming Wang*, Yao-Wei Huang, Greg Sun, I-Da Chiang,., "High-efficiency broadband meta-hologram with polarization controlled

dual images," Nano Lett., vol. 14, no. 1, pp. 225–230, Jan. 2014.

[9]Shukoor, Mohammad Abdul and Sukomal Dey. "Wideband Dual-Cut Circular Ring based Linear-Cross and Linear-Circular Polarizing Reflector." 2020 IEEE International IOT, Electronics and Mechatronics Conference (IEMTRONICS) (2020): 1-5.

[10]Shukoor, Mohammad Abdul and Sukomal Dey. "A Simple I-Shaped Wideband Linear-Linear and Linear-Circular Reflective Type Polarizer." 2021 IEEE 19th International Symposium on Antenna Technology and Applied Electromagnetics (ANTEM) (2021): 1-2.

[11]Song K, Liu Y, Luo C, Zhao X. High-efficiency broadband and multiband cross-polarization conversion using chiral metamaterial. J Phys D Appl Phys 2014;47:505104.

[12] Chen H, Wang J, Ma H, Qu S, Xu Z, Zhang A, et al. Ultra-wideband polarization conversion metasurfaces based on multiple plasmon resonances. J Appl Phys2014;115:154504.

[13] Zhang L, Zhou P, Lu H, Chen H, Xie J, Deng L. Ultra-thin reflective metamaterial polarization rotator based on multiple plasmon resonances. IEEE Antennas WirelessPropagat Lett 2015;14:1157–60.

[14]Deng G, Sun H, Lv K, Yang J, Yin Z, Chi B. An efficient wideband cross-polarizationconverter manufactured by stacking metal/dielectric multilayers via 3D printing. JAppl Phys 2020;127:093103.

[15]Pourmand M, Choudhury PK. Wideband THz filtering by graphene-over-dielectric periodic structures with and without MgF2 defect layer. IEEE Access2020;8:137385–94.

[16]Cheng Z, Cheng Y. "A multi-functional polarization convertor based on chiral metamaterial for terahertz",IEEE Antennas WirelessPropagat Lett 2017;18:7617–12.

[17]Xue Yang,Bo Zhang,Jingling Shen."An tunable terahertz polarization converter based on composite metamaterial".Optical and Quantum Electronics, Springer,2019

[18]Jing Zhao , Jing X."Linear-to-circular Polarization Converter Utilizing Double-arc-based Meta surface at Terahertz Frequency". Optics Express, vol.25,2018, pp. 16050-16058.

[19]Feng luo,Feng lan,Li mengW."Multiband terahertz polarization converter based on L shaped meta surface".Optics Express, vol.26,2018, pp. 16032-16033.

[20]Xiangjun Zhang,Sijie Li,et al."Asymmetric dual-band linear-to-circular converter

by bi-layered chiralmetamaterial". International Journal Of RF and Microwave Computer Aided Engineering,Wiley,2019.

[21]A. K. Baghel, S. S. Kulkarni and S. K. Nayak, "Linear-to-Cross-Polarization Transmission Converter Using Ultrathin and Smaller Periodicity Metasurface," in IEEE Antennas and Wireless Propagation Letters, vol. 18, no. 7, pp. 1433-1437, July 2019, doi: 10.1109/LAWP.2019.2919423.

[22]Bao-qin Lin,Wen-zhun Huang,Lin-tao Lv,Jian-xin Guo Shi-qi Huang,Rui Zhu et al."Ultra-wideband Linear-to-Circular Polarization Conversion Realized by an 8-shaped Metasurface". Journal for Plasmonics, Springer,2020.

[23]PAN Wu, SHEN Da-jun, YAN Yan-jun."Design of broadband polarization converter for terahertz waves".Optoelectron. Lett. Vol.14 No.6·0435,2019.

[24]Zhu L, Zhao X, Miao FJ, Ghosh BK, Dong L, Tao BR, et al. Dual-band polarization convertor based on electromagnetically induced transparency (EIT) effect in all dielectric metamaterial. Opt Express 2019;27:12163–7.

[25]Sakib Quader, Jin Zhang, Muhammad Rizwan Akram, and Weiren Zhu,et.al. "Graphene-Based High Efficiency Broadband Tunable Linear to Circular Polarization Converter for Terahertz Waves".IEEE Journal Of Selected Topics In Quantam Electronics, VOL. 26, NO. 5,2020.

[26]Babar,Jingdong,et.al. A Broad Band BROAD Polarization Converting Metasurface For C and X-Band Applications,IEEE Xplore 2021.

[27]M. A. Shukoor and S. Dey, "Wideband Dual-Cut Circular Ring based Linear-Cross and Linear-Circular Polarizing Reflector," 2020 IEEE International IOT, Electronics and Mechatronics Conference (IEMTRONICS), 2020, pp. 1-5.

[28]Bilal RMH, Saeed MA, Choudhury PK, Baqir MA, Kamal W, Ali MM, et al. Elliptical metallic rings-shaped fractal metamaterial absorber in the visible regime. Sci Repts 2020;10:14035.

[29]M. Ismail Khan1, Zobaria Khalid,FarooqA.Tahir,"Linear and circular-polarization conversion in X-band using anisotropic metasurface", Nature,2019.

[30]Thanh Nghia Cao, Minh Tam Nguyen,Ngoc Hieu Nguyen, Chi Lam Truong and Thi Quynh Hoa Nguyen,et al. "Numerical design of a terahertz cross polarization converter". Mater Res. Express 8 (2021) 065801.

[31]Z. Xu, H. Sheng, Q. Wang, L. Zhou, and Y. Shen, "Terahertz broadband polariza-

tion converter based on the double-split ring resonator metasurface," SN Appl. Sci., vol. 3, no. 9, 2021.

[32]Y. Li, Zhi chi,Floki., "Achieving wideband linear-to-circular polarization conversion using ultrathin bi-layered metasurfaces," J. Appl. Phys., vol. 117, no. 4, pp. 0–7, 2015.

[33]Y. Jiang, Lei wang,Jiao wang., "Ultra-wideband high-efficiency reflective linear-to-circular polarization converter based on metasurface at terahertz frequencies," Opt. Express, 2017. Vol. 25, Issue 22, pp. 27616-27623, vol. 25, no. 22, pp. 27616–27623, Oct. 2017.

[34]S. Luo, B. Li, A. Yu, J. Gao, X. Wang, and D. Zuo, "Broadband tunable terahertz polarization converter based on graphene metamaterial," Opt. Commun., vol. 413, no. November 2017, pp. 184–189, 2018.

[35]X. Yu, X. Gao, W. Qiao, L. Wen, and W. Yang, "Broadband Tunable Polarization Converter Realized by Graphene-Based Metamaterial," IEEE Photonics Technol. Lett., vol. 28, no. 21, pp. 2399–2402, 2016.

[36]M. Fartookzadeh, "Design of metamirrors for linear to circular polarization conversion with super-octave bandwidth," J. Mod. Opt., vol. 64, no. 18, pp. 1854–1861, 2017.

[37]N. Saju, N. Yohannan, R. Mamman, N. Kunju, M. A. Shukoor and S. Dey "A Simple Wideband Dual-Slotted Circular Ring Based Linear-Circular and Linear-Cross Reflective Type Polarizer for THz Regime," pp. 7–10, 2021.

[38] W. T. Chen, KY Yang, C.M Wanget,G.Sun., "High-efficiency broadband meta-hologram with polarizationcontrolled dual images," Nano Lett., vol. 14, no. 1, pp. 225–230, Jan. 2.

[39] Q. Zheng, C. Guo, and J. Ding, "Wideband metasurface-based reflective polarization converter for linear-to-linear and linear-to-circular polarization conversion," IEEE Antennas Wirel. Propag. Lett., vol. 17, no. 8, pp. 1459–1463, 2018.

[40]X.-F. Zang, S.-J. Liu, H.-H. Gong, Y. Wang, and Y.-M. Zhu, "Dual-band superposition induced broadband terahertz linear-to-circular polarization converter," Journal of the Optical Society of America B, vol. 35, no. 4, p. 950, 2018.

[41]X. Zhang, Y. Zhao, H. Zhang, and H. Ye, "Linear-to-Circular Polarization Converter with Adjustable Bandwidth Realized by the Graphene Transmissive Metasur-

face," Plasmonics, vol. 17, p. 1079-1089, Nov. 2021.

# Publications from this thesis

[1]Mohammad Abdul Shukoor,Tejas Shibu Bini, Nissan Kunju, Sukomal Dey "Wideband Dual Polarized Linear-Circular and Linear-Cross Angular Stable THz Reflective Polarizer Based on Modified Square Loop FSS", Appl.Opt.2022(Accepted)

[2]Mohammad Abdul Shukoor,Tejas Shibu Bini, Nissan Kunju, Sukomal Dey, "Wideband Linear-Circular and Linear-Cross Angular Stable THz Reflective Polarizer Based on Circular Ring based FSS,"Optik.(In review)

# Appendix

## High frequency structural simulator (HFSS)

High frequency structural simulator (HFSS) is a commercial electromagnetic structure solver developed by Ansys. HFSS can be used to analyze designs like real life scenarios. The versatile solvers and an intuitive GUI that help to analyze 3D EM (Electro Magnetic) problems. Ansys thermal, structural and fluid dynamics tools along with HFSS provide a powerful and complete multi physics analysis of electronic products, ensuring their thermal and structural reliability. HFSS is synonymous with gold-standard accuracy and reliability for tackling 3D EM challenges under its automatic adaptive meshing technique and sophisticated solvers, which can be accelerated through high performance computing (HPC) technology. The Ansys HFSS simulation suite consists of a comprehensive set of solvers to address diverse electromagnetic problems from passive IC components to extremely large-scale EM analyses. Its reliable automatic adaptive mesh refinement helps create the best mesh and provides high accuracy than all other EM simulators. HFSS can be used to find out various parameters like reflectances,PCR,AR etc. The user interface of HFSS is so simple that anyone with basic knowledge can design and simulate structures.

## Simulation using ANSYS HFSS

The proposed unit cell is generated using a Finite Element Method based (FEM) solver based ANSYS HFSS. There are various steps for simulation in ANSYS HFSS.

1. Geometry of unit cell

   A unit cell is designed using the ANSYS HFSS,fig(5.1).

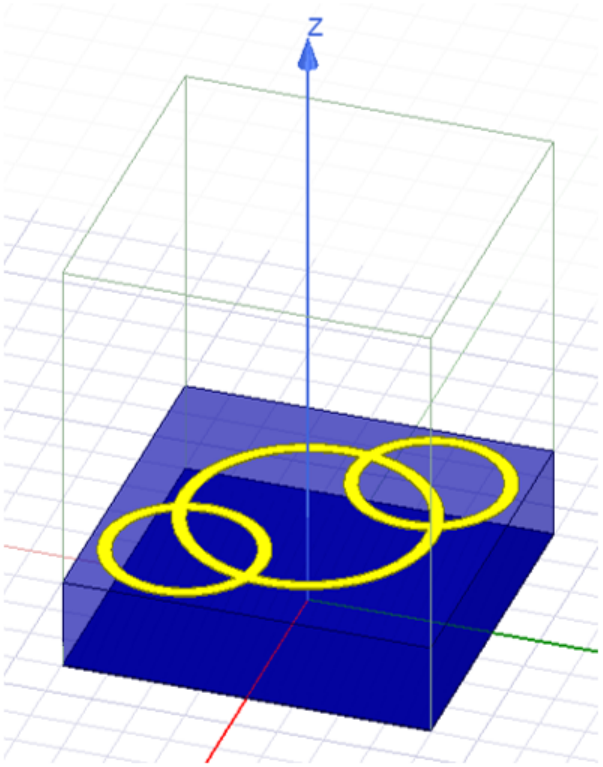


Figure 5.1: Geometry of Unit cell.

2. Boundary conditions

   Boundary conditions are assigned by assigning the master-slave boundary condition. Master-slave boundaries are used to model unit cell of periodic structures. Master and save boundaries are always paired. Fields on the master surface are mapped to the slave surface with a phase shift enforcing a periodicity in the fields.Master-slave conditions are assigned to opposite faces, fig(5.2)

3. Excitation

   Floquet port excitation is given on the top face. Floquet port is used to excite and terminate waves propagating down the unit cell. These are always linked to master or slave boundaries. Floquet port is only used for surfaces exposed to the background. It also replaces radiation boundary and PML for free space field absorption. Floquet port decomposes the fields into floquet modes i.e., Set of TE and TM modes in which the power travels,fig(5.3).

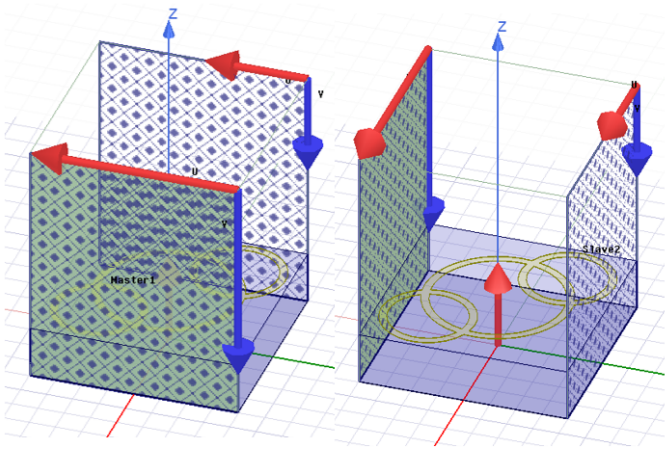


Figure 5.2: Master-slave boundaries conditions are applied.

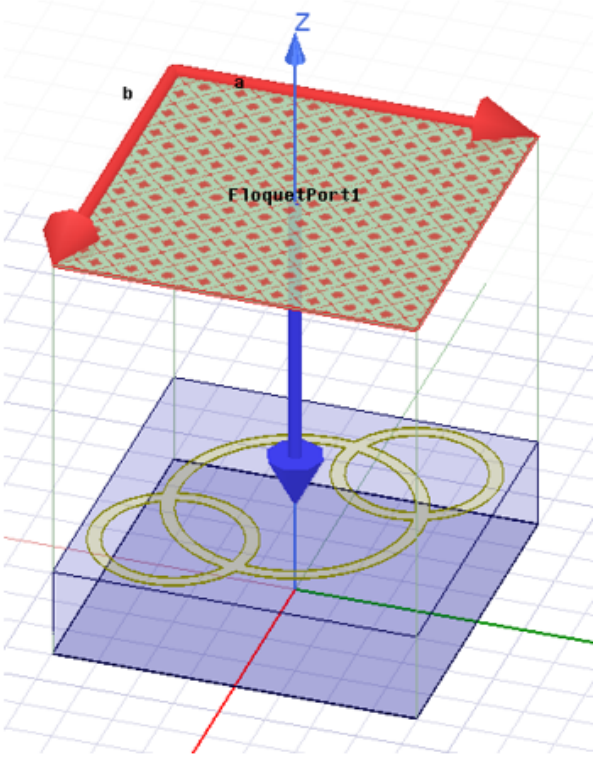


Figure 5.3: Excitation of unit cell using floquet port.